AD-A081 122 OHIO STATE UNIV COLUMBUS ELECTROSCIENCE LAB F/G 17/9
A PHYSICAL OPTICS APPROACH TO THE ELECTROMAGNETIC FIELD SCATTER--ETC(U)
NOV 77 D J RYAN N00530-76-C-0186
UNCLASSIFIED ESL-(78)4428-2 NL

1 OF 1
AD A081122

END
DATE FILMED
3-80
DDC

PHOTOGRAPH THIS SHEET

ADA081122

DTIC ACCESSION NUMBER

II

LEVEL

INVENTORY

ESL (78)4428-2

DOCUMENT IDENTIFICATION

Contract No. N60530-76-C-0186, Dtd. Nov. 1977

DISTRIBUTION STATEMENT A
Approved for public release;
Distribution Unlimited

DISTRIBUTION STATEMENT

ACCESSION FOR		
NTIS	GRA&I	X
DTIC	TAB	☐
UNANNOUNCED		☐
JUSTIFICATION		
Per Ltr. on file		
BY		
DISTRIBUTION /		
AVAILABILITY CODES		
DIST	AVAIL AND/OR SPECIAL	
A		

DISTRIBUTION STAMP

DTIC
ELECTE
S FEB 27 1980 D
D

DATE ACCESSIONED

DATE RECEIVED IN DTIC

PHOTOGRAPH THIS SHEET AND RETURN TO DTIC-DDA-2

DTIC FORM OCT 79 70A

DOCUMENT PROCESSING SHEET

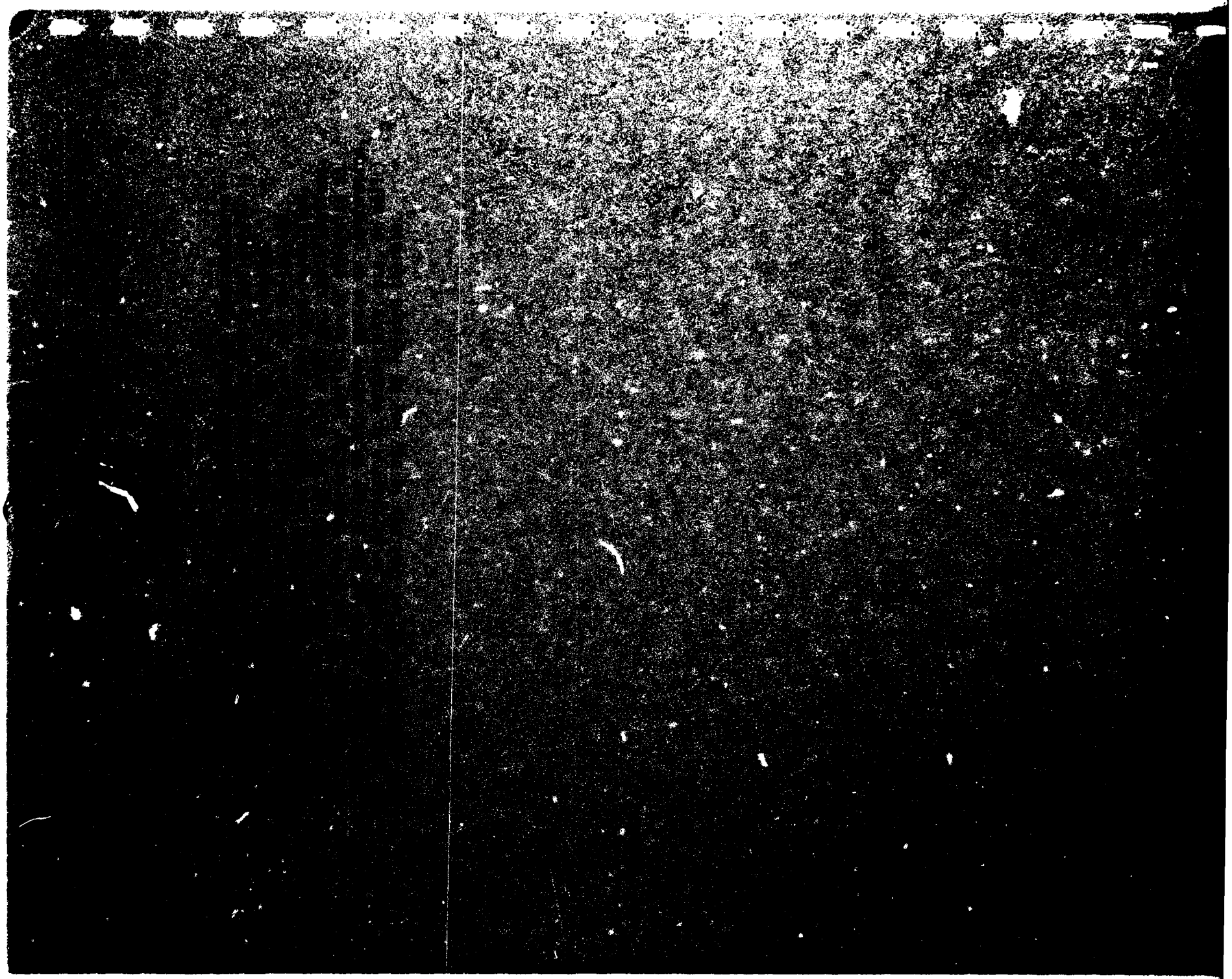

UNCLASSIFIED

SECURITY CLASSIFICATION OF THIS PAGE (When Data Entered)

REPORT DOCUMENTATION PAGE

READ INSTRUCTIONS BEFORE COMPLETING FORM

1 REPORT NUMBER	2 GOVT ACCESSION NO. / 3 RECIPIENT'S CATALOG NUMBER
4 TITLE (and Subtitle): A PHYSICAL OPTICS APPROACH TO THE ELECTRO-MAGNETIC FIELD SCATTERED BY SIMPLIFIED SHIP-SEA MODELS	5 TYPE OF REPORT & PERIOD COVERED: Technical
	6 PERFORMING ORG. REPORT NUMBER: ESL (78)4428-2
7 AUTHOR(s): Daniel J. Ryan	8 CONTRACT OR GRANT NUMBER(s): N60530-76-C-0186
9 PERFORMING ORGANIZATION NAME AND ADDRESS: The Ohio State University ElectroScience Laboratory, Department of Electrical Engineering Columbus, Ohio 43212	10 PROGRAM ELEMENT, PROJECT, TASK AREA & WORK UNIT NUMBERS: Project 3310-0421-76
11 CONTROLLING OFFICE NAME AND ADDRESS: Department of the Navy, Supply Officer, Code 2524 Naval Weapons Center China Lake, California 83555	12 REPORT DATE: November 1977 13 NUMBER OF PAGES: 63
14 MONITORING AGENCY NAME & ADDRESS (if different from Controlling Office)	15 SECURITY CLASS. (of this report): Unclassified 15a DECLASSIFICATION DOWNGRADING SCHEDULE

16 DISTRIBUTION STATEMENT (of this Report)

DISTRIBUTION STATEMENT A
Approved for public release; Distribution Unlimited

17 DISTRIBUTION STATEMENT (of the abstract entered in Block 20, if different from Report)

18 SUPPLEMENTARY NOTES

19 KEY WORDS (Continue on reverse side if necessary and identify by block number)

Composite model	Backscattered field	Geometrical Theory of Diffraction
Physical optics	Gravity waves	
One-dimensional model	Capillary waves	
Ship-sea corner	Cylindrical surface	

20 ABSTRACT (Continue on reverse side if necessary and identify by block number)

A technique is presented to calculate the backscattered field from a simplified ship-sea model with the sea represented by a one-dimensional composite surface, and the ship by a flat plate. The physical optics approximation was used to obtain an expression for the received voltage as a single integral over the profile of the surface. Four principle scattering mechanisms of the model were examined independently to show their effect on the radar return. A composite signature was then

DD FORM 1 JAN 73 1473 EDITION OF 1 NOV 65 IS OBSOLETE

UNCLASSIFIED

SECURITY CLASSIFICATION OF THIS PAGE (When Data Entered)

20.

calculated for several model geometries. The calculated signatures were compared with measured signatures and good agreement was obtained. In all signatures the ship model return could be distinguished from the return due to the other scattering mechanisms.

ACKNOWLEDGMENTS

The author wishes to express his sincere gratitude to Professor William H. Peake, the author's graduate advisor and project supervisor, for his help and guidance throughout this work. Special thanks are also extended to Dr. W. D. Burnside and Mr. John Huang for their patience and helpful suggestions and to Dr. L. Peters, Jr. for his reading of the manuscript. The assistance and cooperation of all the people at the ElectroScience Laboratory is greatly appreciated.

The work reported in this thesis was supported in part by Contract N60530-76-C-0186 between Naval Weapons Center, China Lake, California, and The Ohio State University Research Foundation.

The material contained in this report is also used as a thesis submitted to the Department of Electrical Engineering, The Ohio State University as partial fulfillment for the degree Master of Science.

TABLE OF CONTENTS

CHAPTER I
INTRODUCTION

In past years, research has provided a great deal of information about the mechanics of scattering of an electromagnetic field from the sea surface. Much of this work has been motivated by the problem of detection of ships at sea. This report uses a simplified ship-sea model to obtain some insight into the interaction between the sea and a ship when they are illuminated with a radar signal.

The simplified sea model used in this report is a one-dimensional composite model developed during a previous study [1,2], in which the method of moments and physical optics were used to calculate the scattering from the surface.

This report expands on this previous work by adding a metal flap to represent a simplified model for the ship. Since this combined ship-sea model is too large for the method of moments approach, this report further develops the physical optics approach to study the scattered fields. The first section describes the surface and sets up the geometry of the model. Then a general equation for bistatic scattering from the composite surface is developed. The subsequent sections treat in detail the principal scattering mechanisms, namely; scattering directly back from the composite surface; scattering from the surface-flap corner; and scattering from the edge of the flap. In this report, only horizontal polarization is considered.

CHAPTER II
COMPOSITE SEA SURFACE - SHIP MODEL

The purpose of this section is to describe a simplified one-dimensional model for a ship on the ocean. The ocean is represented by a composite surface made of aluminum roofing. A large scale sinusoid is used to model the gravity waves, and small trapezoids superimposed on the sinusoid are used to model the capillary waves. The ship is modeled by a flat metal plate placed at one end of the model sea surface, (see Figure 1-1).

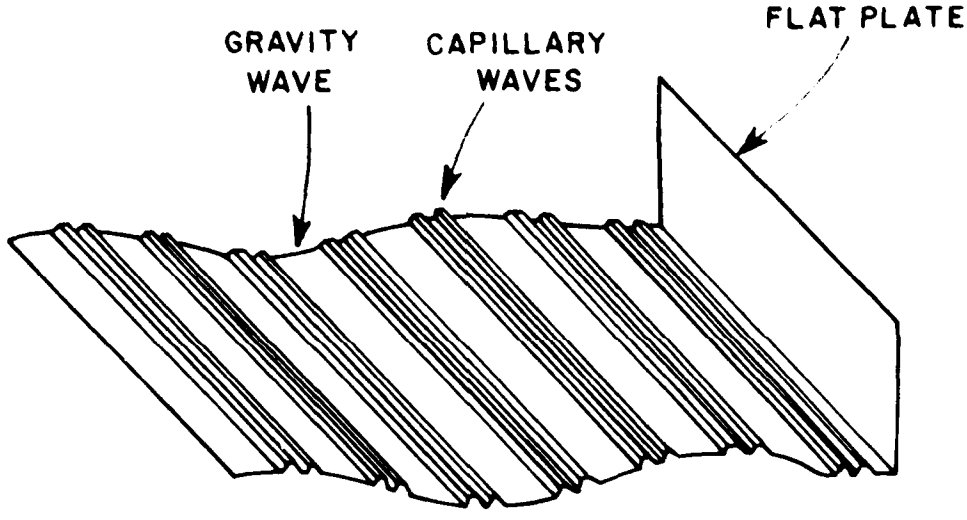

Figure 1-1. Composite sea surface-ship model.

For the actual surface, designed to simulate the sea surface at S-band, the sinusoidal gravity waves have a peak-to-peak height of 3.5 in., and a mechanical wavelength of 4.1 ft. This provides a mean square slope of about 10^{-2}, representing a relatively calm sea (Figure 1-2). The modeled capillary waves are double trapezoids each one 3 cm long and separated by 1 cm (see Figure 1-3), recurring every 20 cm along the sinusoids. This composite surface model can be easily represented mathematically, facilitating the theoretical analysis of the scattered fields.

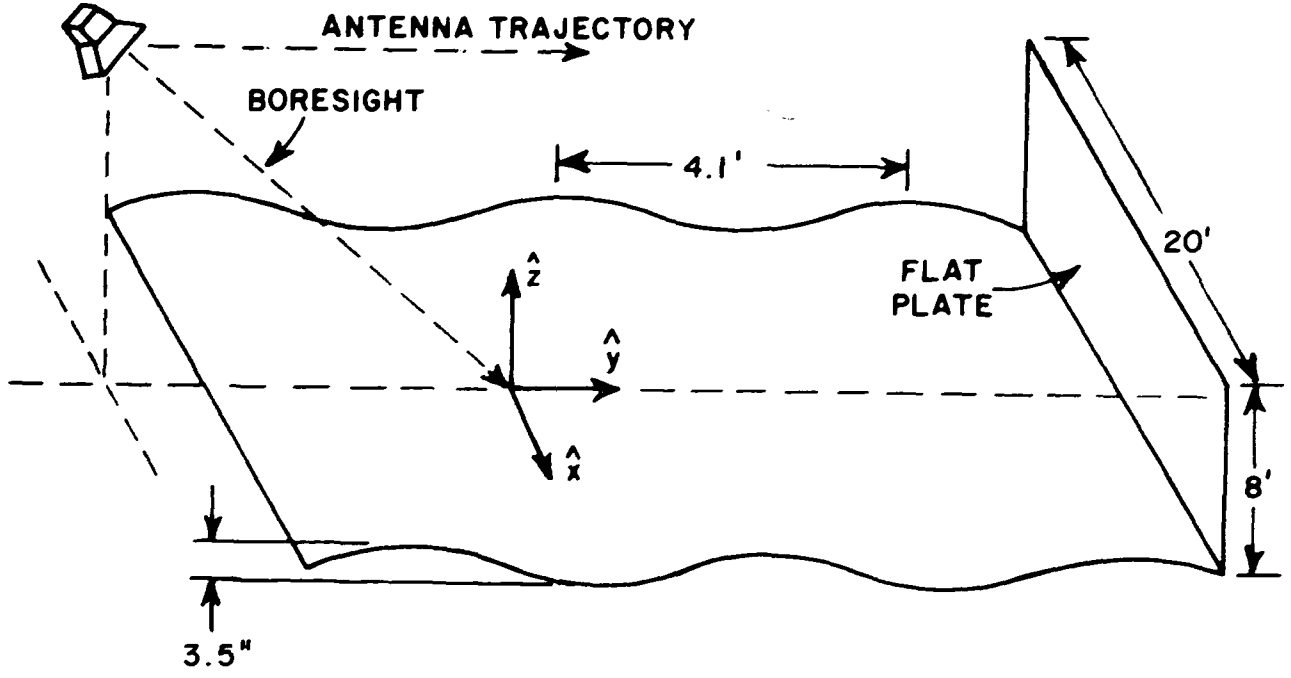

Figure 1-2. Geometry of the cylindrical surface with flat plate.

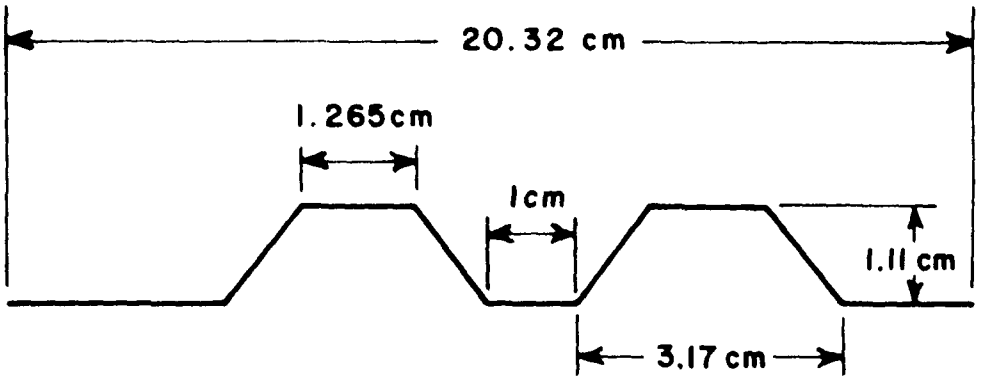

Figure 1-3. Geometry of double trapezoid capillary wave profile.

At one end of the surface model is an eight foot high metal plate representing the ship. This metal plate makes an angle with the surface such that a corner, not necessarily right-angled, is formed. The major contribution to the backscattering from such a configuration is the double-bounce reflection from this corner. For an actual ship at sea, there are a multitude of double and triple bounce corners on the structure of the ship itself. Even so, the largest single contribution to the return signature will probably still be the corner where the ship meets the sea surface.

The ship-sea model described here has four principal mechanisms which give significant contributions to the backscattered field. These are the backscatter from gravity waves, backscatter from the trapezoids, backscatter from the ship-sea double bounce region, and the diffracted field from the plate edge. First we shall consider the general physical optics formulation for this one-dimensional geometry, and then investigate the scattering from each of the four mechanisms. The calculated scattered fields will be compared with the experimental results obtained at the Encounter Simulation Laboratory, where the ship-sea model shown in Figure 1-1 was constructed.

CHAPTER III
PHYSICAL OPTICS EXPRESSION FOR SCATTERING FROM A CYLINDRICAL SURFACE

The first step in obtaining the scattered fields is to calculate the scattering from an arbitrary cylindrical surface. The approach taken here is to use the physical optics currents generated by the incident field and then find the far field radiated by these current generators.

The general equations for the physical optics currents, given the incident field, were summarized in Reference [1]. The scattered electric field, $d\vec{E}_s$, at a point in the far-field of a current element $\vec{J}_s$ is given by

$$d\vec{E}_s = jkZ_o \frac{e^{-jkR'_n}}{4\pi R'_n} (\vec{J}_s \times \hat{r}'_n) \times \hat{r}'_n \, ds \tag{1}$$

where $\hat{r}'_n$ is the unit vector describing the direction for R'_n, the distance from the surface element ds to the field point, k is the wave number and $Z_o = 120\pi$ ohms. The surface current $\vec{J}_s$, in the physical optics approximation, is

$$\vec{J}_s = 2\hat{n} \times \vec{H}_i \tag{2}$$

where $\hat{n}$ is the normal to the surface element ds (see Figure 3-1) and is given by

$$\hat{n} = -\sin\phi \, \hat{y} + \cos\phi \, \hat{z}. \tag{3}$$

The angle between the normal $\hat{n}$ and the vertical is defined to be ϕ.

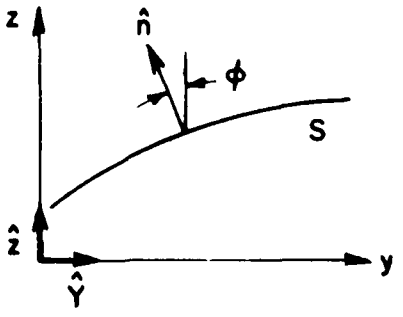

Figure 3-1. Geometry of the normal to the surface.

The magnetic field $\vec{H}_i$ incident upon the surface can be written as

$$\vec{H}_i = I_o (f_v f_h)^{1/2} \vec{p}_h \frac{e^{-jkR_n}}{R_n} \tag{4}$$

where I_o is a nominal current strength, and f_v, f_h are antenna pattern factors, to be discussed later. For an antenna of maximum gain, G_T, which radiates power P_T

$$I_o = (P_T G_T / 4\pi Z_o)^{1/2} \quad . \tag{5}$$

The polarization state of the transmitted field is characterized by a polarization factor $\vec{p}_h$. For horizontal (perpendicular) polarization the electric field $\vec{E}_o$, in the aperture, is in the x_o direction (see Figure 3-2). For the geometry of the sea-ship model, the unit vector x_o is parallel to the coordinate unit vector $\hat{x}$. The polarization factor can be expressed as

$$\vec{p}_h = - \frac{\hat{x}_o \times \hat{r}_n}{|\hat{x}_o \times \hat{r}_n|} \quad . \tag{6}$$

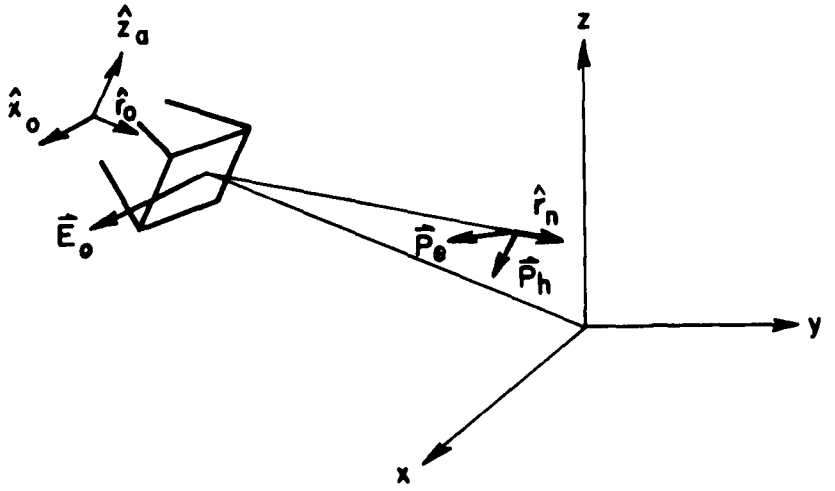

Figure 3-2. Polarization state for the transmitted field.

The one way antenna power pattern, $F(\xi,\eta)$, is assumed to be a product pattern with one principal plane in the x-y plane (pattern angle η) and the other principal plane containing the z axis (pattern angle ξ) (see Figure 3-3), so that $F(\xi,\eta)$ can be written as

$$f(\xi,\eta) = f_v(\xi)f_h(\eta) \quad . \tag{7}$$

By assuming that $f_h(\eta)$ is Gaussian, it will later be possible to reduce the two dimensional surface integration to a one dimensional integration.

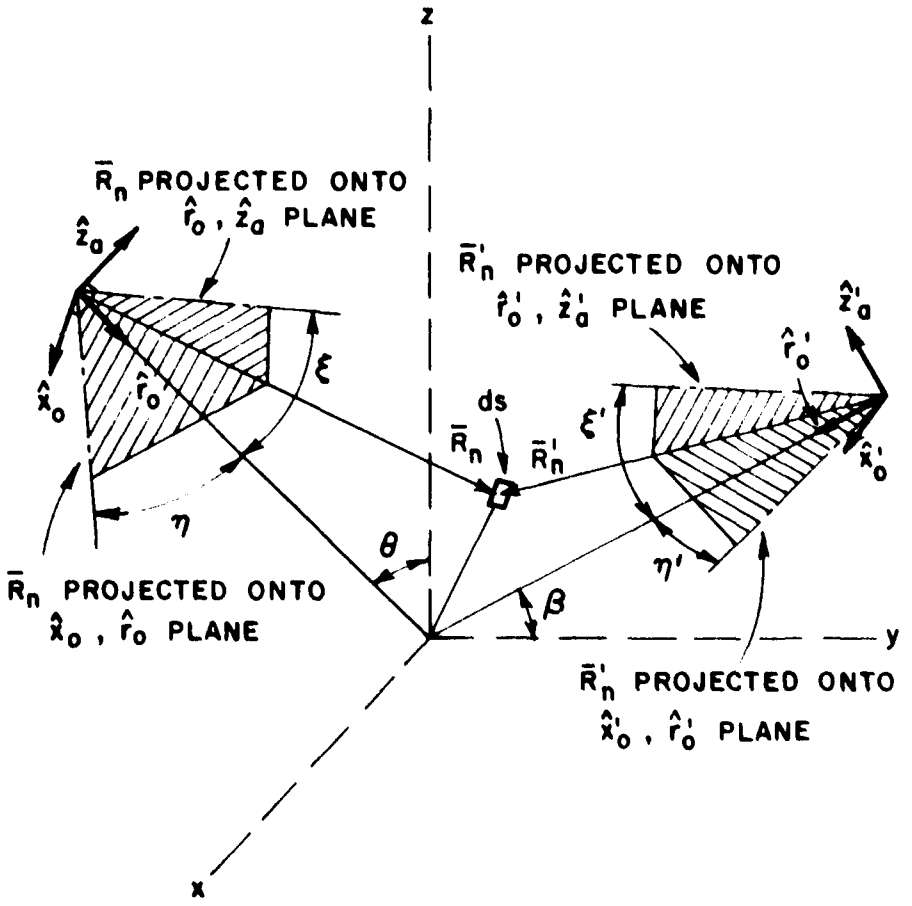

Figure 3-3. Transmitter and receiver coordinate angles.

Combining Equations (2) and (4) gives an expression for the physical optics currents.

$$\vec{J}_s = 2\, I_o\, f(\xi,\eta)^{1/2}\, \frac{e^{-jkR_n}}{R_n}\, (\hat{n} \times \vec{P}_h) \tag{8}$$

Substituting the equations for $\hat{n}$ (Equation (3)) and $\vec{P}_n$ (Equation (6)) into Equation (8) gives

$$\vec{J}_s = 2I_o\, f(\xi,\eta)^{1/2}\, \frac{e^{-jkR_n}}{R_n} \left[(-\sin\phi\, \hat{y} + \cos\phi\, \hat{z}) \times \frac{-(\hat{x} \times \hat{r}_n)}{|\hat{x} \times \hat{r}_n|} \right] . \tag{9}$$

From Figure 3-4 we have that

$$\hat{r}_n = \frac{1}{R_n} (R_o \hat{r}_o + y\hat{y} + h\hat{z} + x\hat{x}) \tag{10}$$

where

$$\hat{r}_o = \sin\theta\, \hat{y} - \cos\theta\, \hat{z} \quad .$$

Substituting Equation (10) back into the equation for the physical optics current (Equation (9)) and simplifying, we obtain

$$\vec{J}_s = 2I_o\, f(\xi,\eta)^{1/2}\, \frac{e^{-jkR_n}}{R_n}\, \frac{(R_o\cos(\theta-\phi) + y\sin\phi - h\cos\phi)}{[(R_o\cos\theta - h)^2 + (R_o\sin\theta + y)^2]^{1/2}}\, \hat{x} . \tag{11}$$

For the antenna polarization chosen here, the physical optics currents are in the x-axis direction.

Using the expression (11) for $\vec{J}_s$, in Equation (1), and expanding the triple cross product

$$(\hat{x} \times \hat{r}'_n) \times \hat{r}'_n = \left(\frac{x^2}{R'^2_n} - 1\right)\hat{x} + \frac{x}{R'^2_n}(y - R'_o\cos\beta)\hat{y} - \frac{x}{R'^2_n}(h - R'_o\sin\beta)\hat{z} \tag{12}$$

where the unit vector $\hat{r}'_n$ is defined in Figure 3-4,

$$\hat{r}'_n = \frac{1}{R'_n}[(y - R'_o\cos\beta)\hat{y} + (h - R'_o\sin\beta)\hat{z} + x\hat{x}) \tag{13}$$

we obtain

$$d\vec{E}_s = \frac{2jkZ_o}{4\pi} I_o f(\xi,\eta)^{1/2} \frac{e^{-jk(R_n + R'_n)}}{R_n R'_n} \tag{14}$$

$$* \frac{(R_o\cos(\theta-\phi) + y\sin\phi - h\cos\phi)}{[(h - R_o\cos\theta)^2 + (R_o\sin\theta - y)^2]^{1/2}}$$

$$* \left\{\left(\frac{x^2}{R'^2_n} - 1\right)\hat{x} + \frac{x}{R'^2_n}(y - R'_o\cos\beta)\hat{y} - \frac{x}{R'^2_n}(h - R'_o\sin\beta)\hat{z}\right\}$$

$$* \frac{d_x d_y}{\cos\phi} \quad .$$

So far, only the transmitting antenna pattern has been accounted for. The receiver, at the point where the field is being measured, must also have a power pattern and a polarization direction. We shall assume in this case that the receiving antenna has the same pattern as the transmitting antenna. Also, to find the horizontally polarized component of the scattered field, we assume that the receiving antenna polarization is in the x-direction. Equation (14) can be changed to take into account the receiving antenna by multiplying by the one way power pattern, given by (see Figure 3-3)

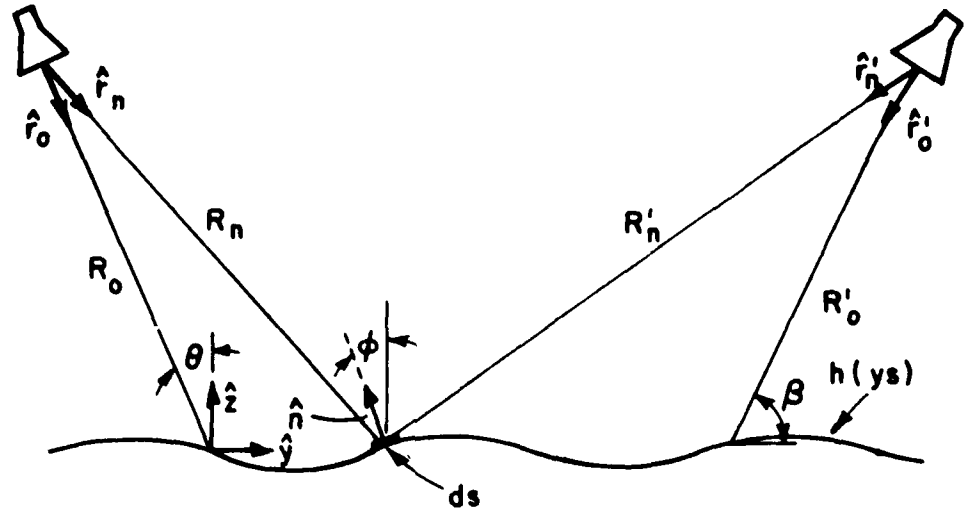

Figure 3-4. Incident and reflected ray geometry.

$$f(\xi',\eta')^{1/2} = f_v(\xi')^{1/2}\, f_n(\eta')^{1/2} \tag{15}$$

and by taking the dot product with the receiver polarization

$$\hat{a}_r = \hat{x} \quad .$$

Furthermore, if the maximum receiving aperture of the antenna is given by A_e, the receiver voltage, i.e., the voltage at the receiver due to the scattered field from ds, is found to be

$$dV_r = \frac{2jV_o}{4\pi}\, f(\xi,\eta)^{1/2}\, f(\xi',\eta')^{1/2}\, \frac{e^{-jk(R_n + R'_n)}}{R_n R'_n} \tag{16}$$

$$* \left(\frac{x^2}{R'^2_n} - 1\right) \frac{(R_o\cos(\theta-\phi) + y\sin\phi - h\cos\phi)}{[(h-R_o\cos\theta)^2 + (y+R_o\sin\theta)^2]^{1/2}}\, \frac{d_x d_y}{\cos\phi}$$

where

$$V_o = Z_o I_o (A_e k^2)^{1/2} \quad .$$

Equation (16) gives an expression for the horizontally polarized component of the electric field at a point, scattered from an incremental area of the total surface. To obtain the total field at any point, a double integration over the entire surface is required.

Assuming that both the receiver and the transmitter have a Gaussian product pattern, then

$$f(\xi,\eta)^{1/2} = e^{-\frac{1}{2} A \tan^2\eta} \; e^{-\frac{1}{2} B \tan^2\xi}$$

$$f(\xi',\eta')^{1/2} = e^{-\frac{1}{2} A \tan^2\eta'} \; e^{-\frac{1}{2} B \tan^2\xi'} \qquad (17)$$

where A and B are beamwidth parameters. The angles ξ,η,ξ' and η' (shown in Figure 3-3) can be expressed analytically in terms of dot products.

$$\tan\xi = \frac{\hat{r}_n \cdot \hat{z}_a}{\hat{r}_n \cdot \hat{r}_o} = \frac{y\cos\theta + h\sin\theta}{R_o + y\sin\theta - h\cos\theta} \qquad (18)$$

$$\tan\eta = \frac{\hat{r}_n \cdot \hat{x}}{\hat{r}_n \cdot \hat{r}_o} = \frac{x}{R_o + y\sin\theta - h\cos\theta} \qquad (19)$$

$$\tan\xi' = \frac{\hat{r}'_n \cdot \hat{z}'_a}{\hat{r}'_n \cdot \hat{r}'_o} = \frac{h\cos\beta - y\sin\beta}{R'_o - y\cos\beta - h\sin\beta} \qquad (20)$$

$$\tan\eta' = \frac{\hat{r}_n' \cdot \hat{x}'}{\hat{r}_n' \cdot \hat{r}_o'} = \frac{x}{R_o' - y\cos\beta - h\sin\beta} \qquad (21)$$

Substituting these angle definitions back into Equation (16) gives the following expression for the received voltage.

$$V_r = \frac{2jV_o}{4\pi} \int_y \int_x \frac{(R_o\cos(\theta-\phi)+y\sin\phi-h\cos\phi)}{\cos\phi[(h-R_o\cos\theta)^2+(y+R_o\sin\theta)^2]^{1/2}} \left(\frac{x^2}{R_n'^2} - 1\right) \frac{e^{-jk(R_n'+R_n)}}{R_n' R_n} \qquad (22)$$

$$* \; e^{-\frac{A}{2}x^2\left(\frac{1}{R_2^2} + \frac{1}{R_2'^2}\right)} \; e^{-\frac{B}{2}(y\cos\theta+h\sin\theta)^2/R_2^2} \; e^{-\frac{B}{2}(h\cos\beta-y\sin\beta)^2/R_2'^2} \; dx\,dy$$

where

$$R_2 = R_o + y\sin\theta - h\cos\theta$$

$$R_2' = R_o' - y\cos\beta - h\sin\beta \quad .$$

Because of the choice of the two principal planes defining the power patterns, we are able to separate the x and y integrations. By integrating from minus infinity to infinity in the x direction, we can integrate analytically the x dependent part of the double integral so that

$$V_r = \frac{2jV_o}{4\pi} \int_y \bar{X} \; \frac{(R_o\cos(\theta-\phi) + y\sin\phi-h\cos\phi)}{\cos\phi[(h-R_o\cos\theta)^2 + (y+R_o\sin\theta)^2]^{1/2}} \qquad (23)$$

$$* \; e^{-\frac{B}{2}(y\cos\theta+h\sin\theta)^2/R_2^2} \; e^{-\frac{B}{2}(h\cos\beta-y\sin\beta)^2/R_2'^2} \; dy$$

where

$$\underline{X} = \int_{-\infty}^{\infty} \left(\frac{x^2}{R_n'^2} - 1 \right) \frac{e^{-jk(R_n + R_n')}}{R_n R_n'} \; e^{-\frac{A}{2}\left(\frac{1}{R_2^2} + \frac{1}{R_2'^2} \right) x^2} \, dx$$

and

$$R_n^2 = R_1^2 + x^2$$

$$R_n'^2 = R_1'^2 + x^2 \tag{24}$$

with

$$R_1^2 = (h - R_o \cos\theta)^2 + (y + R_o \sin\theta)^2$$

$$R_1'^2 = (h - R_o' \sin\beta)^2 + (y - R_o' \cos\beta)^2 \tag{25}$$

Using the Fresnel approximation in expanding the exponential phase terms

$$e^{-jkR_n} = e^{-jk(R_1^2 + x^2)^{1/2}} \cong e^{-jk\left(R_1 + \frac{x^2}{2R_1}\right)}$$

$$e^{-jkR_n'} = e^{-jk(R_1'^2 + x^2)^{1/2}} \cong e^{-jk\left(R_1' + \frac{x^2}{2R_1'}\right)} \tag{26}$$

and approximating the denominator terms as

$$\frac{1}{R_n} = \frac{1}{(R_1^2 + x^2)^{1/2}} \cong \frac{e^{-\frac{x^2}{2R_1^2}}}{R_1}$$

$$\frac{1}{R_n'^3} = \frac{1}{(R_1'^2 + x^2)^{3/2}} \cong \frac{e^{-\frac{3x^2}{2R_1'^2}}}{R_1'^3} \quad , \tag{27}$$

the evaluation of the $\underline{\bar{X}}$ integral in Equation (23) gives

$$\underline{\bar{X}} = \frac{-R_2 R_2' \sqrt{2\pi}\, e^{-jk(R_1+R_1')}}{[AR_1^2 R_1'^2 R_2'^2 + AR_1^2 R_1'^2 R_2^2 + jkR_1 R_1'^2 R_2^2 R_2'^2 + jkR_1' R_1^2 R_2^2 R_2'^2 + R_1'^2 R_2^2 R_2'^2 + 3R_1^2 R_2^2 R_2'^2]^{1/2}} \tag{28}$$

Further evaluation of the integral, Equation (23), would require a computer. Notice also that if Equation (23) is evaluated by computer, any desired vertical plane antenna patterns, $f_V(\xi)$ and $f_V(\xi)$, may be used in place of the gaussian patterns of Equation (17).

CHAPTER IV
BACKSCATTER FROM A MODEL SEA SURFACE

As pointed out in Section II, there are four principal mechanisms contributing to the total field scattered by the simplified ship-sea model. We consider first the backscatter from the large-scale (gravity) waves.

A. Geometry of the Wave Models

To calculate this direct backscatter from the gravity waves, we first define the surface. The gravity wave model lies in the x-y_s plane. The surface height is a function of y_s only, so that

$$h(y_s) = H_{ei} + H_{ei} * \sin(w_m * y_s + \text{Phase}) \qquad (29)$$

and the surface is uniform in the x direction. The constant H_{ei} is the peak amplitude of the sinusoid, $w_m = \frac{2\pi}{\lambda_m}$ is the mechanical wavenumber of the surface. The surface itself is 40 feet in length, with $\lambda_m = 4.1$ feet and $H_{ei} = 1.75$ inches. In implementing the computations of the scattered field, the surface is assumed to occupy the range $-40<y_s<0$ with the flat plate position at $y_s=0$.

The capillary waves, modeled by small trapezoids, are superimposed on the surface of the gravity waves. Each trapezoid is made up of plane segments as shown in Figure 2-3. The upper three segments represent the actual surface. The other two segments are straight line approximations to the original sinusoid.

The scattering from such a composite surface could be computed from Equation (23) since the profile $h(y_s)$ of the surface is known. However, in order to simplify subsequent calculations, the three upper segments of each trapezoid are considered to be individual scatterers. That is, instead of integrating over the surface of the trapezoid, we consider the current density, J_s, concentrated at the center of each of the segments. These current densities are then used to determine the field scattered from the segments. If any trapezoids are positioned such that a face is in the shadow region of the incident field, then the current density on that segment is taken to be zero. In addition, since the field scattered from the sinusoidal component alone (i.e., no trapezoids) is computed first, in order to illustrate the effect of the gravity waves, the total field may be found by adding the field scattered by the trapezoids to this gravity

wave field. Thus the fields scattered by the two lower segments of the individual trapezoid must be subtracted from the total field to account for the fact that the interval of the sinusoidal profile, $h(y_s)$, occupied by the trapezoid has already been computed in the gravity wave program.

B. Discussion of Computer Code for Backscatter from the Sinusoidal Surface (Gravity Waves)

Since the profile of the surface is known, the voltage at the receiver due to the field scattered from the model surface is found by a numerical integration of Equation (23). The Equation then takes the form

$$V_r = \frac{-jV_o}{2\pi} \sum_{y=Y_{s1}}^{Y_{s2}} \frac{R_2 R_2' R_o}{R_1} (\cos\theta + \sin\theta\tan\phi + y/R_o\tan\phi - h(y_s)/R_o) \quad (30)$$

$$* g^{-1/2} e^{-jk(R_1+R_1')} e^{-\frac{B}{2}(\tan^2\xi+\tan^2\xi')} \Delta y$$

where

$$g = AR_1^2R_1'^2R_2'^2 + AR_1^2R_1'^2R_2^2 + jkR_1R_1'^2R_2^2R_2'^2 + jkR_1'R_1^2R_2^2R_2'^2 + R_1'^2R_2^2R_2'^2 + 3R_1^2R_2^2R_2'^2 .$$

The variables in Equation (30) are shown in Figure 4-1, and are defined as follows.

The boresight distance, R_o, is the distance from the radar to the y-axis, measured along the radar axis. R_o is given by

$$R_o = zz/\sin(\pi/2 - \theta)$$

where zz is the perpendicular height of the radar above the y-axis. The return boresight distance R_o' is equal to R_o since the radar is monostatic. The incremental value, Δy, is the width (measured horizontally) of the portion of the surface contributing to the sum in Equation (30). There is just one physical optics current element per increment. In the program of the Appendix, y is taken to be 0.01.

By taking the origin of the x,y,z coordinate system to be at the intersection of the boresight with the y-axis, the distance between the radar and the surface point at Δy, R_1, can be written as

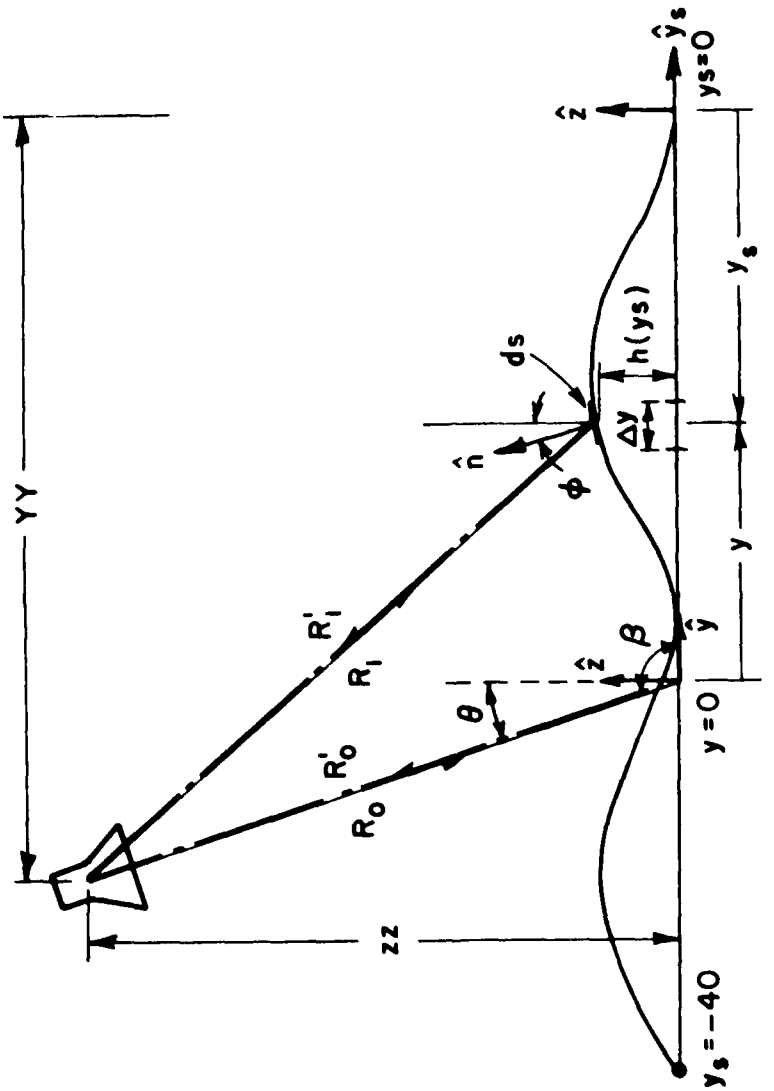

Figure 4-1. Geometry for backscatter from gravity waves.

$$R_1^2 = (y + R_o \sin\theta)^2 + (h(y_s) - R_o \cos\theta)^2$$

$$= (y - y_o)^2 + (h(y_s) - h_o)^2 \qquad (31)$$

where θ is the angle between the vertical (z) axis and the boresight, and

$$y_o = - R_o \sin\theta$$

$$h_o = zz = R_o \cos\theta \quad .$$

The return distance between the radar and Δy is R_1' and is equal to R_1 for direct backscatter. The quantity R_2 is the projection of R_1 onto R_o and is defined as

$$R_2 = R_o + y \sin\theta - h(y_s) \cos\theta \quad . \qquad (32)$$

R_2' is the projection of R_1' onto R_o' and is given by

$$R_2' = R_o' - y \cos\beta - h(y_s) \sin\beta \qquad (33)$$

where the angle β is measured between the horizontal (y) axis and the return boresight. The quantities R_2 and R_2' are also equal for a monostatic radar.

The portion of the surface contributing to the sum is defined by the limits $y=Y_{s1}$ and $y=Y_{s2}$. These limits are determined by the angles at which the incident field is 20 dB down from the boresight level. Since we have defined the point $y=0$ to be at the intersection of the boresight with the y-axis, the value of Y_{s1} will be negative and Y_{s2} positive. The surface profile function $h(y_s)$ is always evaluated with respect to the origin of the x,y_s,z coordinate system, that is $y_s=0$ at the end of the surface model (see Figure 4-2). We then have for the limits of integration

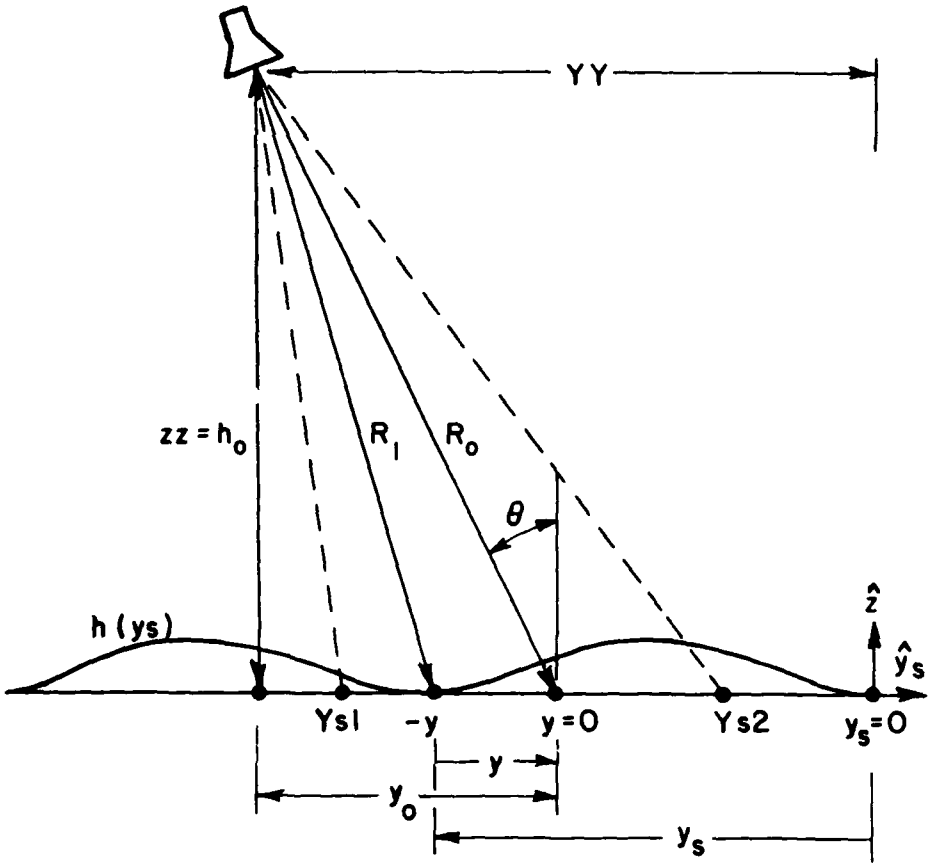

Figure 4-2. Geometry defining the limits of integration.

$$Y_{s1} = y_o + h_o \cdot \tan(\theta - 1.3 * \theta_{3dB})$$

$$Y_{s2} = y_o + h_o \cdot \tan(\theta + 1.3 * \theta_{3dB}) \qquad (34)$$

where θ_{3dB} is the 3dB beamwidth in degrees, which for our gaussian pattern has been taken to be 15°.

The specified section of the computer code in the Appendix utilizes Equation (30) with $h(y_s)$ defined by Equation (29) to calculate the receiver voltage due to the backscattered field from the sinusoidal surface model, as the radar moves from the end of the surface at y_s=-40 to the flat plate at y_s=0. This portion of the code

requires input values of; the height, Dl in feet, of the radar above the y axis at y_s=0, the look angle, α, of the radar as measured from the trajectory to boresight in degrees, and the dive angle, ψ, of the radar in degrees from the horizontal. The output is the voltage at the receiver (complex valued) in units of volts (see Figure 4-3).

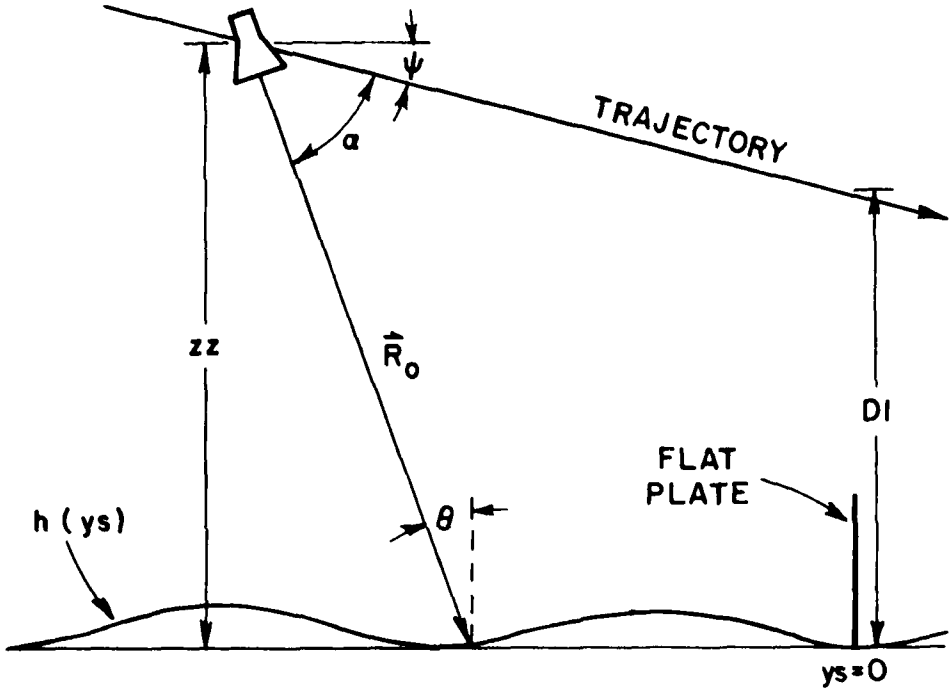

Figure 4-3. Geometry of input variables.

C. Discussion of Computer Code for Backscatter from Trapezoids (Capillary Waves)

The most direct way to include the physical optics scatter from the trapezoids would be to superimpose their profile on the profile given by $h(y_s)$ for the gravity waves, and apply Equation (30). However, it is possible to generate a set of equations that adequately describe the scattering from a single, arbitrarily placed trapezoid, so that one set of equations could be used in a computer code to calculate the backscatter from all of the trapezoids.

The field scattered from an arbitrary trapezoid is found by considering each segment of the trapezoid separately. The field contributions from the three upper segments are added together. Because the field from the entire sinusoidal surface has already been calculated, the scattering from those portions which are now covered must be subtracted from the total field. For this reason the field contribution from the bottom two segments is subtracted from the field of the upper three segments. The net field contribution from the five segments is added to the field scattered from the gravity wave. This process is repeated for each trapezoid on the surface. When the radar is moved to a new position a new value for the received complex voltage is calculated. In this manner, a backscattering signature for the model sea surface is obtained for the specified radar trajectory.

To find the net backscattered field due to a trapezoid, we consider first the field scattered from one side of the trapezoid by using a simplified form of Equation (23). Because each side of the trapezoid profile is only a small fraction of a wavelength long, we can further simplify the calculation of the scattered field by considering the entire physical optics current to be concentrated in the center of the segment. Thus, no integration in the y-direction along the segment is needed. Instead we simply multiply by the effective width of the segment. Also, since we are dealing with a monostatic radar, the transmitted and received distances are equal, eliminating the primes on variables which denote the scattered distances, and doubling the transmitted distances. Equation (23) can now be written in a form suitable for calculations of the field scattered from the trapezoids.

$$V_r(n) = -\frac{jV_o}{2\pi} \frac{L(n)\sin\alpha(n)\,(y+R_o\sin\theta) + \cos\alpha(n)\,(h-R_o\cos\theta)}{\cos\alpha(n)\left[(h-R_o\cos\theta)^2 + (y+R_o\sin\theta)\right]^{1/2}}\, dwy(n)$$

$$* e^{-B(y\cos\theta+h\sin\theta)^2/R_2^2}$$

$$*\int_{-\infty}^{\infty} \frac{e^{-j2kR_1}}{R_1^2}\, e^{-\left(\frac{2}{R_1^2} + \frac{A}{R_2^2} + j\frac{k}{R_1}\right)x^2}\, dx \qquad (35)$$

where $n=1,\cdots,5$ depending on which segment of the trapezoid is being considered (see Figure 4-4); $L(n)$ is either +1 or -1, depending on the normals n_i

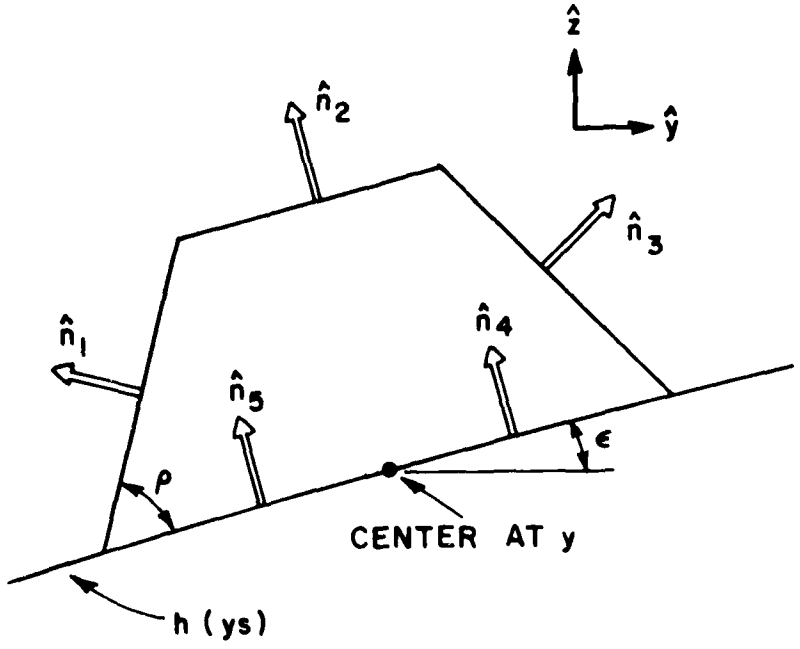

Figure 4-4. Profile of trapezoid showing normals.

$$\hat{n}_i = L(n)\,\sin\sigma(n)\,\hat{y} + \cos\sigma(n)\,\hat{z} \tag{36}$$

$L(n) = -1$ for $n = 1,2,4,5$

$L(n) = +1$ for $n = 3$.

The parameter $\sigma(n)$ is also a function of the segments of the trapezoid.

$$\begin{aligned}
\sigma(1) &= \rho+\epsilon \\
\sigma(2) &= \epsilon \\
\sigma(3) &= \rho-\epsilon \\
\sigma(4) &= \epsilon \\
\sigma(5) &= \epsilon
\end{aligned} \tag{37}$$

Here, θ is the angle describing the slope of the surface $h(y_s)$ at the midpoint of the trapezoid, and ϕ is the angle that defines the slope of the sides of the trapezoid (see Figure 4-4). Since ϕ_i defines the slope of the i-th segment of the trapezoid, the width of the i-th segment projected along the y-axis will be a function of ϕ_i, so that

$$\begin{aligned} dwy(1) &= 0.048\cdot\cos(\phi+\theta) \\ dwy(2) &= 0.415\cdot\cos(\theta) \\ dwy(3) &= 0.048\cdot\cos(\phi-\theta) \\ dwy(4) &= 0.052\cdot\cos(\theta) \\ dwy(5) &= 0.052\cdot\cos(\theta) \quad . \end{aligned} \tag{38}$$

By carrying out the integration over x in Equation (35) and summing over the five faces of the trapezoid, an equation for the received voltage contributed from a trapezoid centered at position y can be written

$$V_r = -\frac{jV_0}{2\pi}\sum_{n=1}^{5}(\pm)\frac{L(n)\sin\phi(n)(y+R_0\sin\theta)+\cos\phi(n)(h-R_0\cos\theta)}{\cos\phi(n)[(h-R_0\cos\theta)^2+(y+R_0\sin\theta)^2]^{1/2}}$$

$$\cdot\, dwy(n)\,\frac{e^{-2jkR_1}}{R_1^2}\,\frac{e^{-B(y\cos\theta+h\sin\theta)^2/R_1^2}}{(2/R_1^2+A/R_2^2+jk/R_1)^{1/2}} \qquad (v) \tag{39}$$

where the choice of sign ($\pm$) is such that the top segments (n=1,2,3) are (+) and the bottom two segments (n=4,5) are (-). In this equation y is defined to be the position of the mid-point of the trapezoid on the surface $h(y_s)$. All other terms are as defined for the gravity wave calculations.

The portion of the computer code that calculates the field scattered from the trapezoids is a subroutine in the gravity wave code. This subroutine requires the position of the radar, and returns the voltage at the receiver due to the field scattered from the trapezoid superimposed on $h(y_s)$. This complex voltage is added to the voltage due to scattering from the gravity waves so that the program gives, at each position of the radar, the receiver voltage due to the field scattered from the composite surface model. The following section gives the results of some typical calculations.

D. Results for Backscatter from Surface Model

The signature for the sea-surface model, (i.e., the receiver voltage as a function of the distance YY) as calculated using the physical optics current approximation, is shown in Figure 4-5 for two different trajectory geometries. Two signatures are shown for each configuration, one modeling the sea as a gravity wave alone (i.e., as $h(y_S)$) and the other as the composite surface including the trapezoidal capillary waves. In all signatures, the magnitude of the receiver voltage is in dB below reference voltage V_0, which has been taken to be unity. All signatures are plotted so that they are normalized to the highest value in the signature.

Note that the radar system used to obtain the measured signatures includes a range gate (short or long) to eliminate wall reflections. The effect of this range gate has been included in the calculated signatures by inserting a gating function $C(R_1,1)$ in, e.g. Equations (30) and (39). The argument 1 in $C(R_1,1)$ denotes that the short range gate was used.

Figure 4-5a shows clearly the effects of the periodicity of the sinusoidal surface model. When the contribution of the trapezoids is added in, the signatures take on a more random appearance, but the underlying periodicity is still noticeable (Figure 4-5b). The lobe at the end of the signatures of Figure 4-5a is the result of terminating the surface at $y_S=0$.

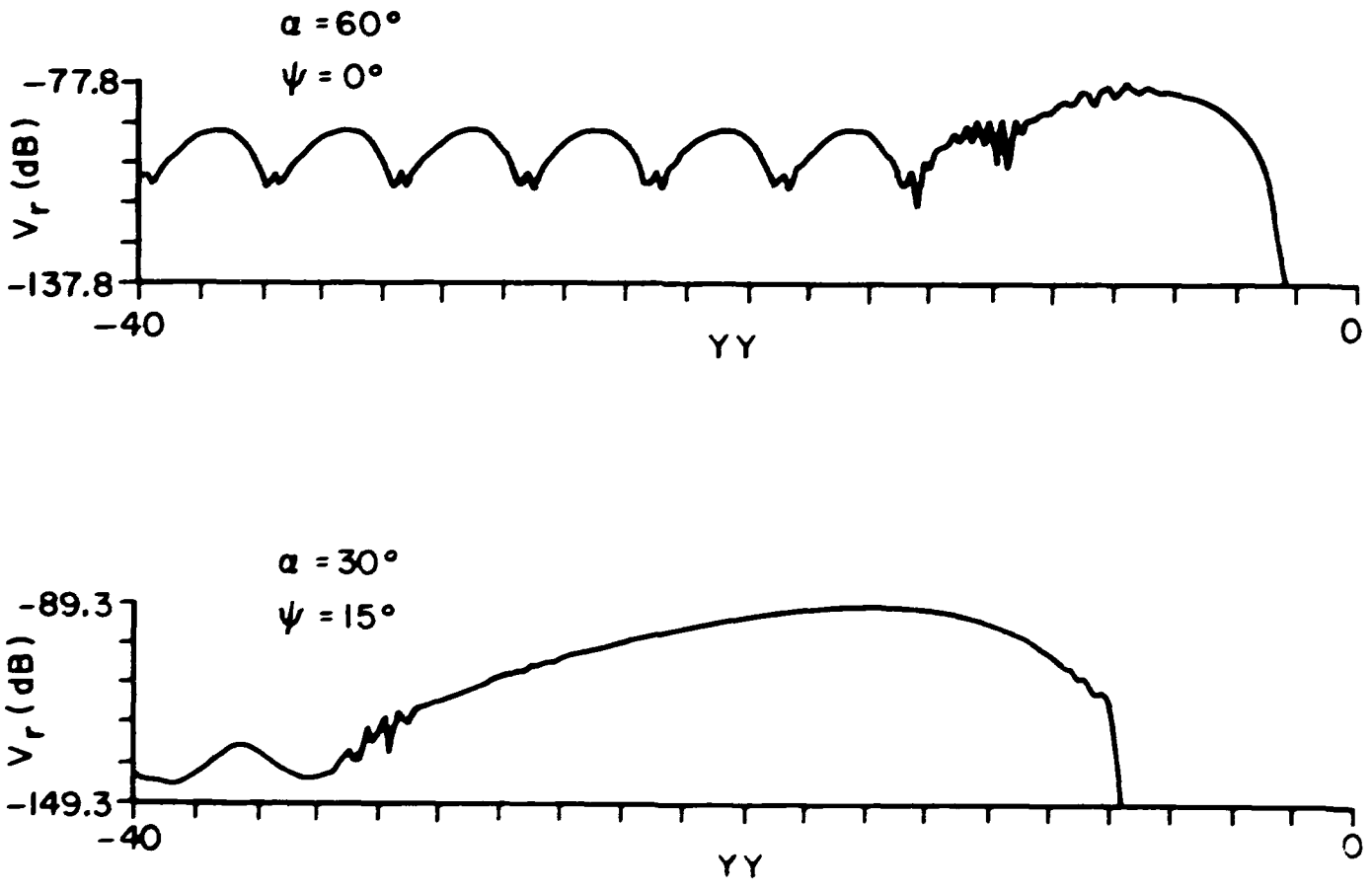

Figure 5-5a. Signatures for backscatter from gravity waves alone.

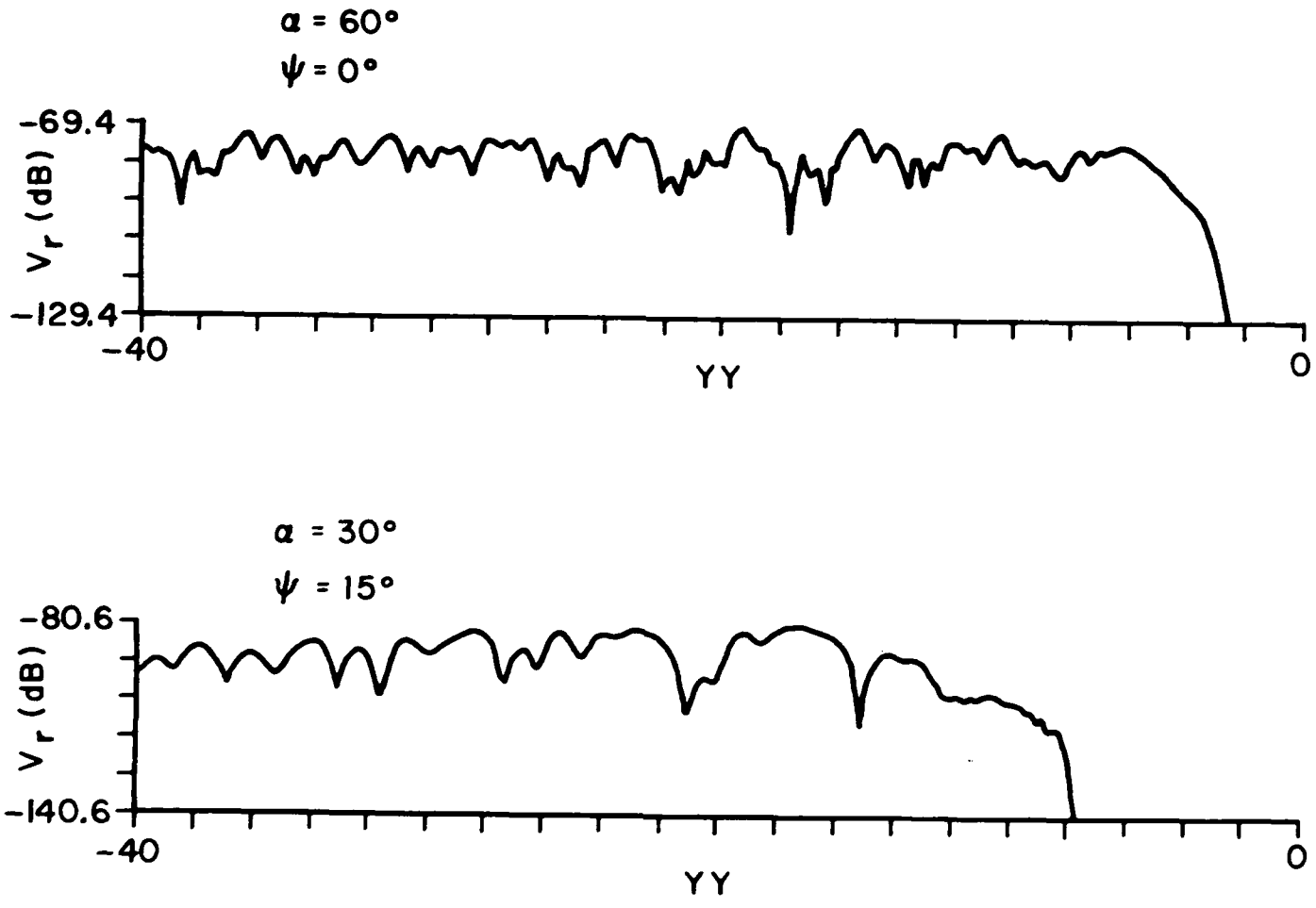

Figure 4-5b. Signatures for backscatter from composite surface.

CHAPTER V
DOUBLE-BOUNCE SCATTER FROM A SHIP MODEL

A. Geometry of the Ship Model

The next scattering mechanism to be considered is the double-bounce corner formed by the intersection of the ship and the sea surface. In the Encounter Simulation Laboratory experiment [3], the ship is modeled by the 8' high plate. To simulate different roll angles for the ship the plate angle μ can be varied. The radar approaches in the yz plane from the negative y direction along a trajectory defined by the dive angle ψ (see Figure 5-1).

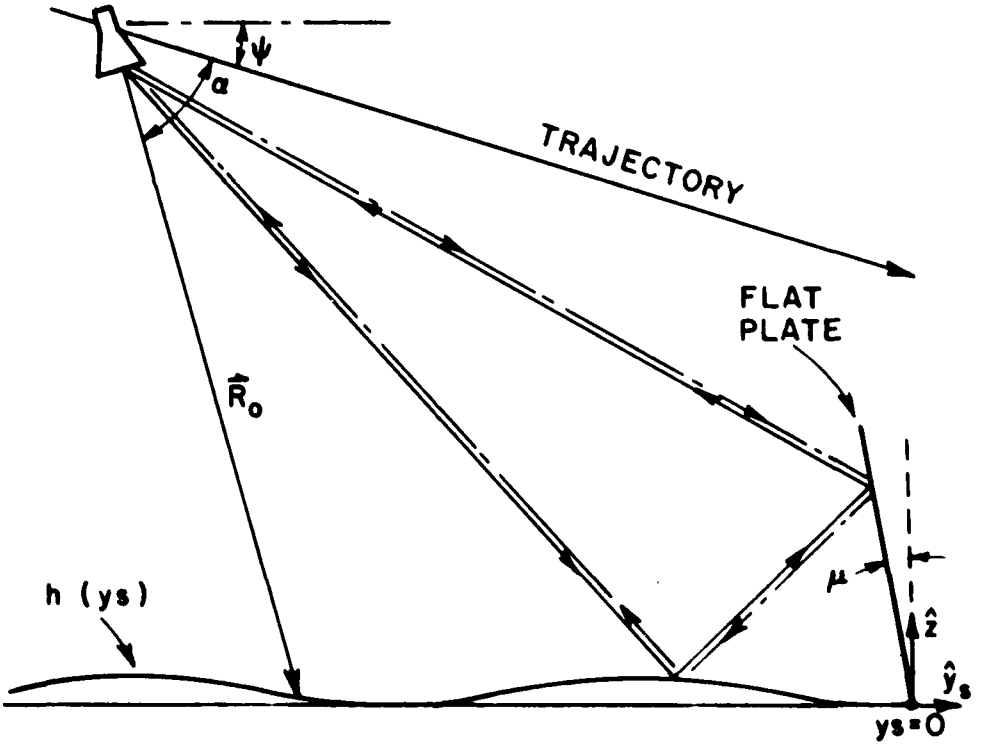

Figure 5-1. Geometry for double-bounce scatter.

B. Simplifications to Model

There are, in fact, two double-bounce paths, one in the direction transmitter-sea surface-plate-receiver and the other in the direction transmitter-plate-sea surface-receiver. In both cases the scatter from the sea surface is in the forward direction. Because the dominant scattering effect from the sea surface is the forward scatter from the large scale structure, $h(y_s)$, we can neglect the effects of the capillary waves in calculating the double-bounce effect. This will greatly simplify the field calculations and the computer code.

Even after neglecting the capillary waves, a direct calculation of the scattered fields would take an unreasonable amount of computer time. Instead we may take advantage of certain symmetries of the problem to further simplify the calculations.

For any configuration of the sea-plate-transceiver positions, the geometry can be made symmetric about the flat plate by using image theory. That is, since the plate is an ideal reflector, we may image the surface and transceiver. By appropriately defining the limits of integration, we can then effectively remove the plate (see Figure 5-2). This can be done, of course, only if the sea surface behind the plate can be neglected. For the study of the double-bounce scatter this is indeed the case. Reflection off the plate is taken into account by multiplying the field passing through the plane of the plate by a minus sign (for horizontal polarization).

Another simplification is that the two ray paths from transmitter to receiver through any point C on the plate are of equal length. Therefore, by reciprocity, we may calculate the field due to a first reflection off the sea, and multiply it by two to account for the ray hitting the plate first. The resulting configuration is shown in Figure 5-3.

Thus, by image theory and reciprocity, the problem has been reduced to a simple application of the equation derived in Section III for bistatic scattering. For a horizontally polarized field

$$V_r = -\frac{2jV_o}{2\pi}\int_Y \frac{R_2R_2'}{R_1}\left(R_o\cos\theta+R_o\sin\theta\tan\phi+y\tan\phi-h(y_s)\right)$$

$$* \; g^{-1/2}\; e^{-jk(R_1+R_1')}\; e^{-\frac{B}{2}(\tan^2\xi+\tan^2\xi')}\; dy \qquad (40)$$

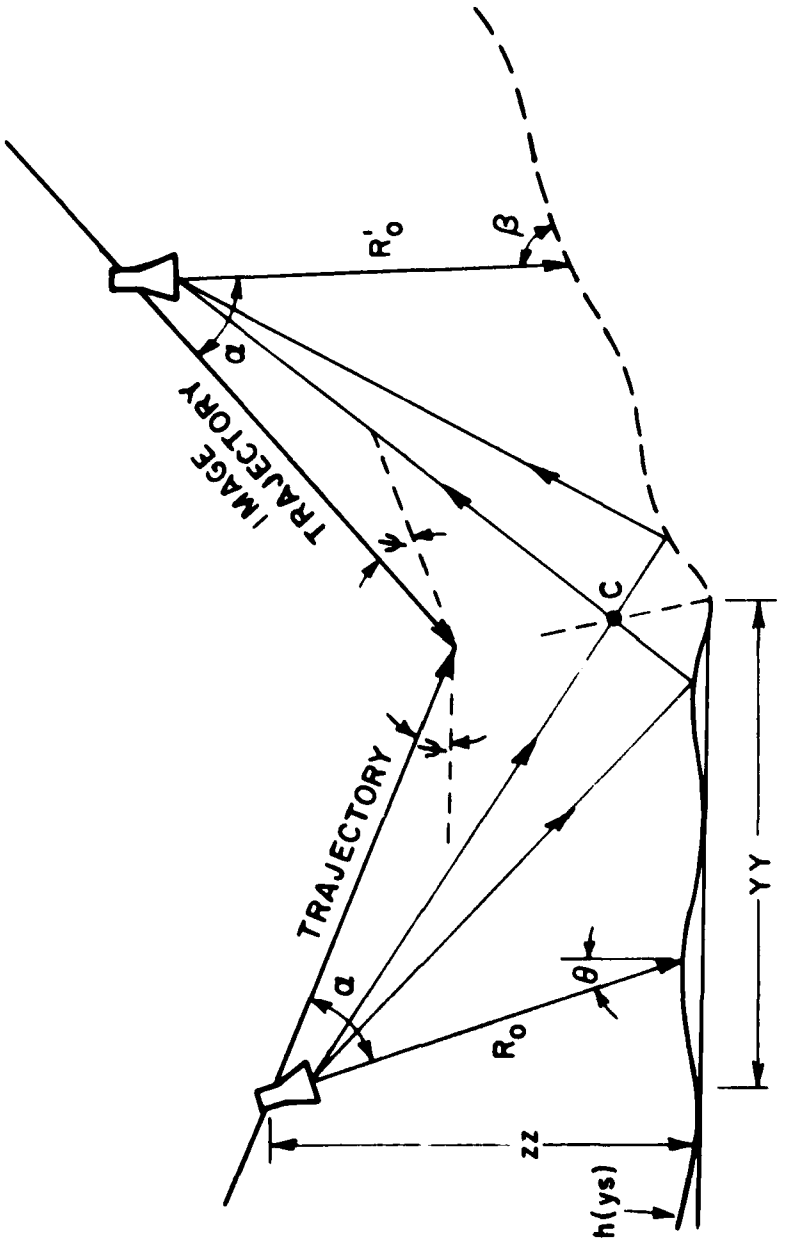

Figure 5-2. Geometry resulting from image theory.

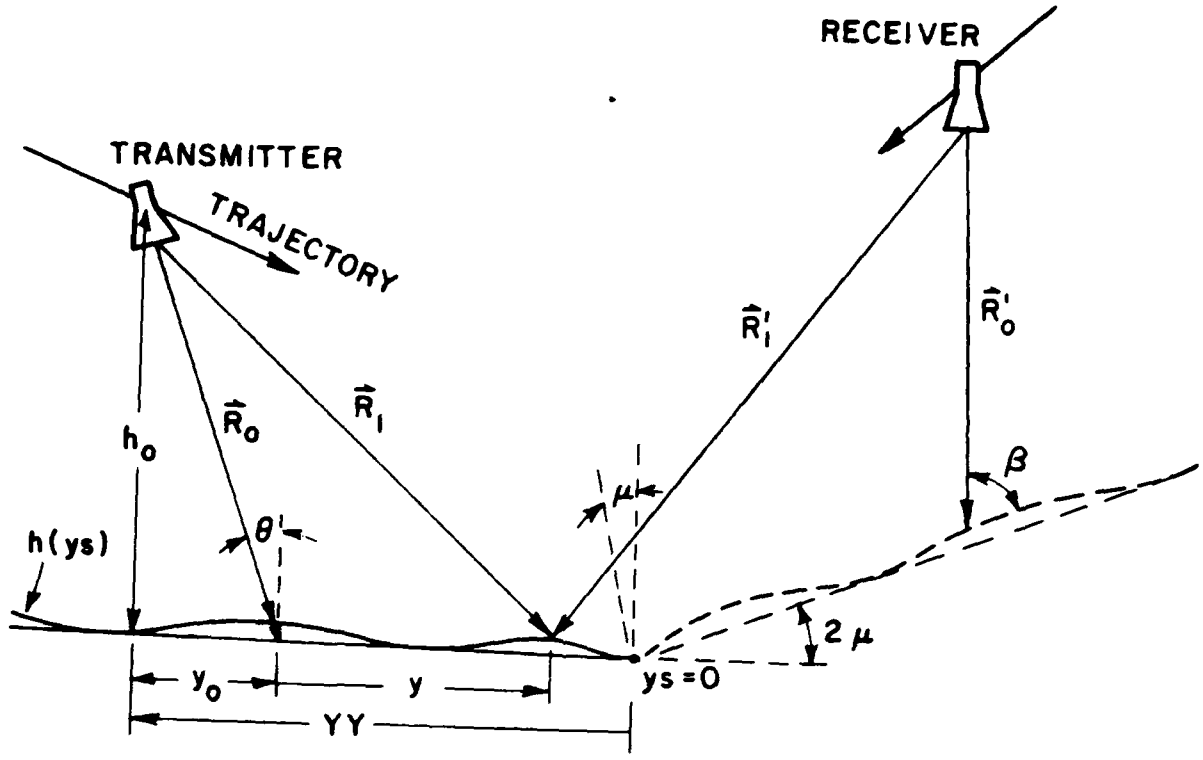

Figure 5-3. Simplified geometry of double-bounce scatter.

where

$$g=AR_1^2R_1'^2R_2'^2+AR_1^2R_1'^2R_2^2+R_1'^2R_2^2R_2'^2+3R_1^2R_2^2R_2'^2+jkR_2^2R_2'^2(R_1'R_1^2+R_1R_1'^2)$$

and $h(y_s)$ is the sinusoid defined by Equation (29). The appropriate limits of integration will be discussed in the next section.

C. Discussion of Computer Code for Double-bounce Scatter

The field which is reflected back to the radar by the presence of the plate can be calculated by a numerical integration of Equation (40). By reducing the integral to a finite summation over small increments, Δy, we have

$$V_r = \frac{2jV_o}{2\pi}\sum_{y_{s1}}^{y_{s2}} \frac{R_2R_2'}{R_1}(R_o\cos\theta+R_o\sin\theta\tan\phi+y\tan\phi-h(y_s))$$

$$* g^{-1/2}\, e^{-jk(R_1+R_1')}\, e^{-\frac{B}{2}(\tan^2\xi+\tan^2\xi')}\,\Delta y \qquad (41)$$

where g is defined in Equation (40). Unlike the formulation of Equation (30) for the scattering due to the gravity waves alone, the primed variables and the unprimed variables are not equal. This is because of the simplifications introduced by the image theory. Figure 5-3 defines the variables for this scattering equation. The terms R_1 and R_1' are the distances from the incremental segment, Δy, on the surface $h(y_s)$ to the transmitter and receiver, respectively. These distances are given by

$$R_1^2 = (y-y_o)^2 + (h-h_o)^2$$

$$R_1'^2 = \left(yy-y + \frac{(yy+y_o)\sin\beta}{\sin(\frac{\pi}{2}-2\mu+\theta)}\right)^2 + (h(y_s) - R_o'\sin\beta)^2 \qquad (42)$$

where the angles β,μ,θ and the quantities y, y_o, yy and h_o are as shown in Figure 5-3. The receiver boresight distance R_o' is

$$R_o' = R_o + (yy+y_o)\sin 2\alpha/\sin(\pi/2-2\alpha+\theta) \qquad (43)$$

where R_o is the boresight distance to the transmitter. The antenna pattern angles θ and θ' are as defined in Section III. The projections R_2 and R_2' are given by

$$R_2 = R_o + y\sin\alpha - h(y_s)\cos\alpha$$

$$R_2' = R_o' - (y-2y_o - 2yy)\cos\alpha - h(y_s)\sin\alpha \quad . \qquad (44)$$

The limits of this numerical integration, Y_{S1} and Y_{S2} are determined by the 20 dB points of the antenna pattern, as for the gravity wave integration, with one additional constraint. The integration must take into account only those ray paths for which either the transmitted ray or the reflected ray passes through the plate. The limits of integration must satisfy both conditions simultaneously (see Figure 5-4).

The calculations of the double-bounce scatter are made in the subroutine DBS. The subroutine requires as input the position of the radar, and size and position of the plate. The subroutine returns to the main program the complex voltage at the receiver due to the reflections from the ship-sea corner back to the radar. The following pages show typical signatures of several double-bounce geometries.

D. Results for Double-bounce Scatter from the Ship Model

The signatures for the double-bounce scatter contribution, as calculated using Equation (41), are shown in Figure 5-5 for several different model geometries. The magnitude of the receiver voltage, in dB below the reference voltage V_o, is plotted as a function of the position yy of the radar. As before, a range gate function $C[(R_1+R_1')/2,1]$ must be included in Equation (41).

The effect of the depression angle α can be seen by comparing the signatures of Figure 5-5a or 5-5b. Note that for near-grazing incidence angles the double-bounce contribution extends over a greater range. The effect of the dive angle ψ can be seen by comparing the signature with $\alpha=60°$ and $\psi=5°$ in Figure 5-5b with the signature in Figure 5-5c that has the same α and ψ. A larger dive angle results in a signature less extended in range and shifted in position towards yy=0.

Comparing the signatures of Figure 5-5c illustrates the effect of the plate angle μ. The radar return becomes stronger over a wider range for obtuse corner angles ($\mu<0.$), and decreases in magnitude with compressed range for acute corner angles ($\mu>0.$).

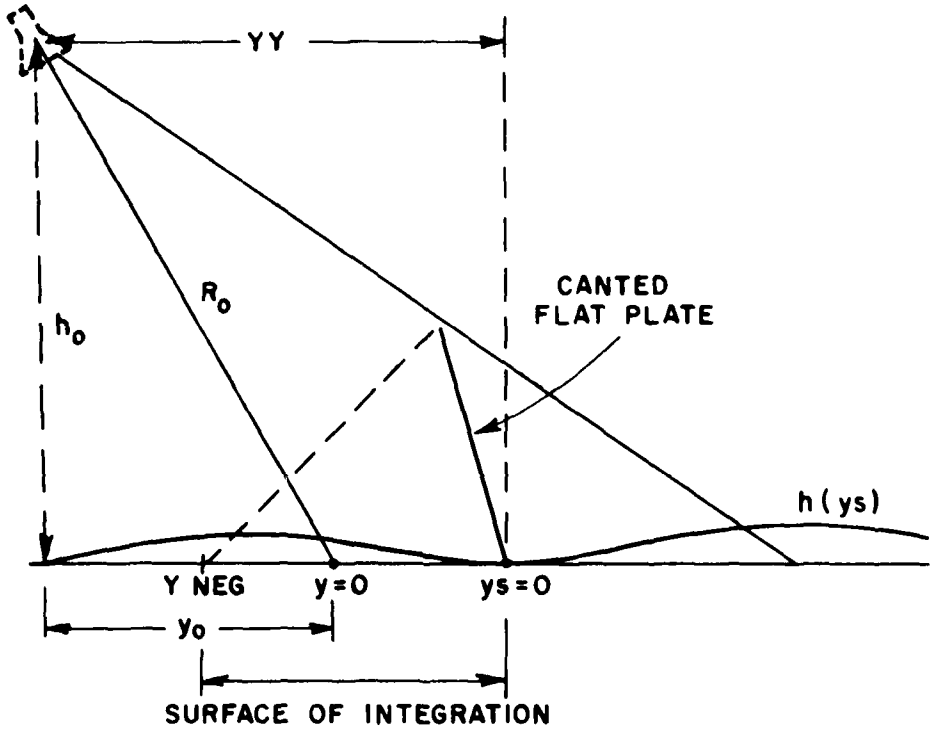

Figure 5-4. Geometry for defining the surface of integration.

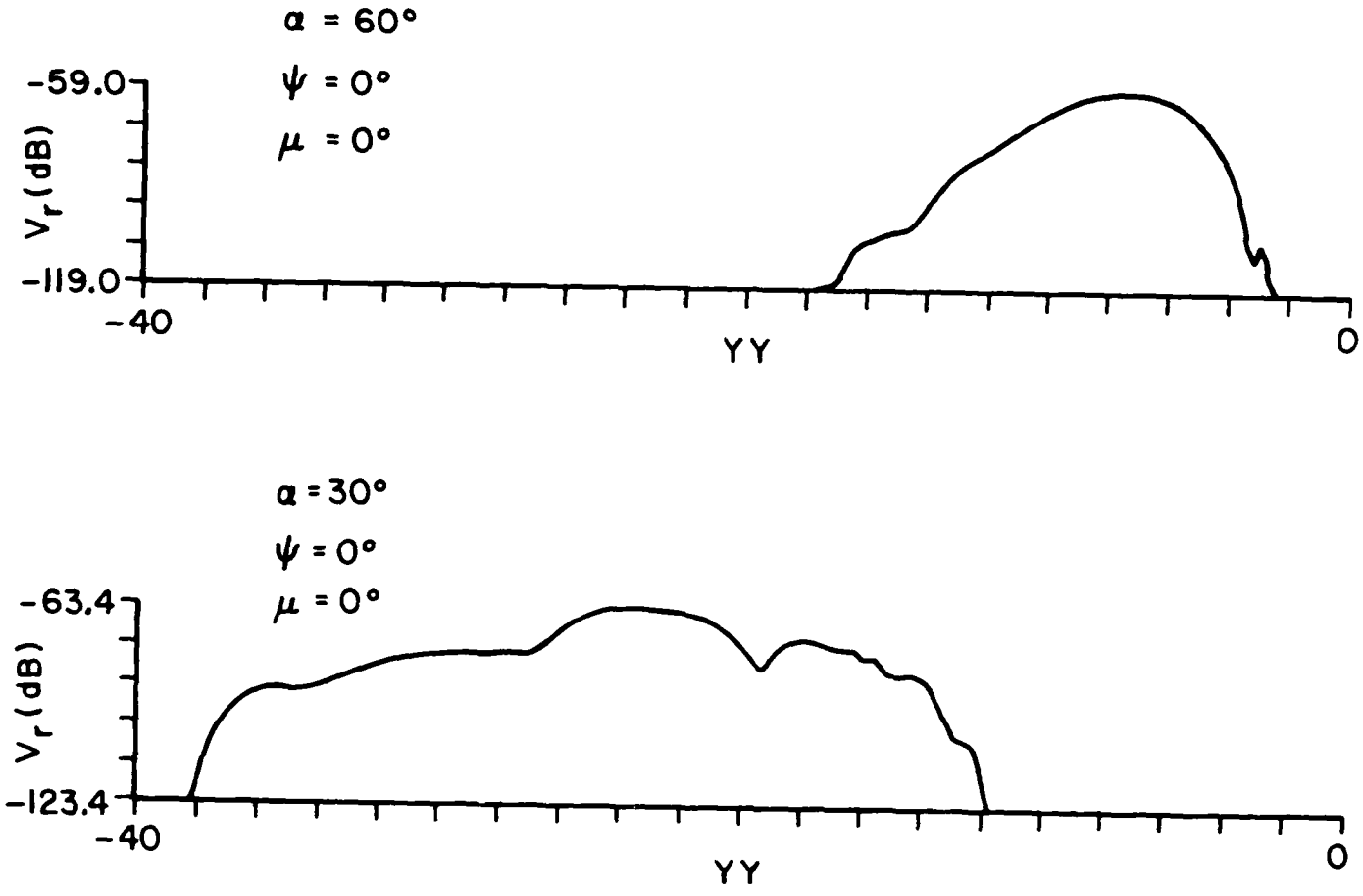

Figure 5-5a. Signatures for double-bounce scatter from a ship model.

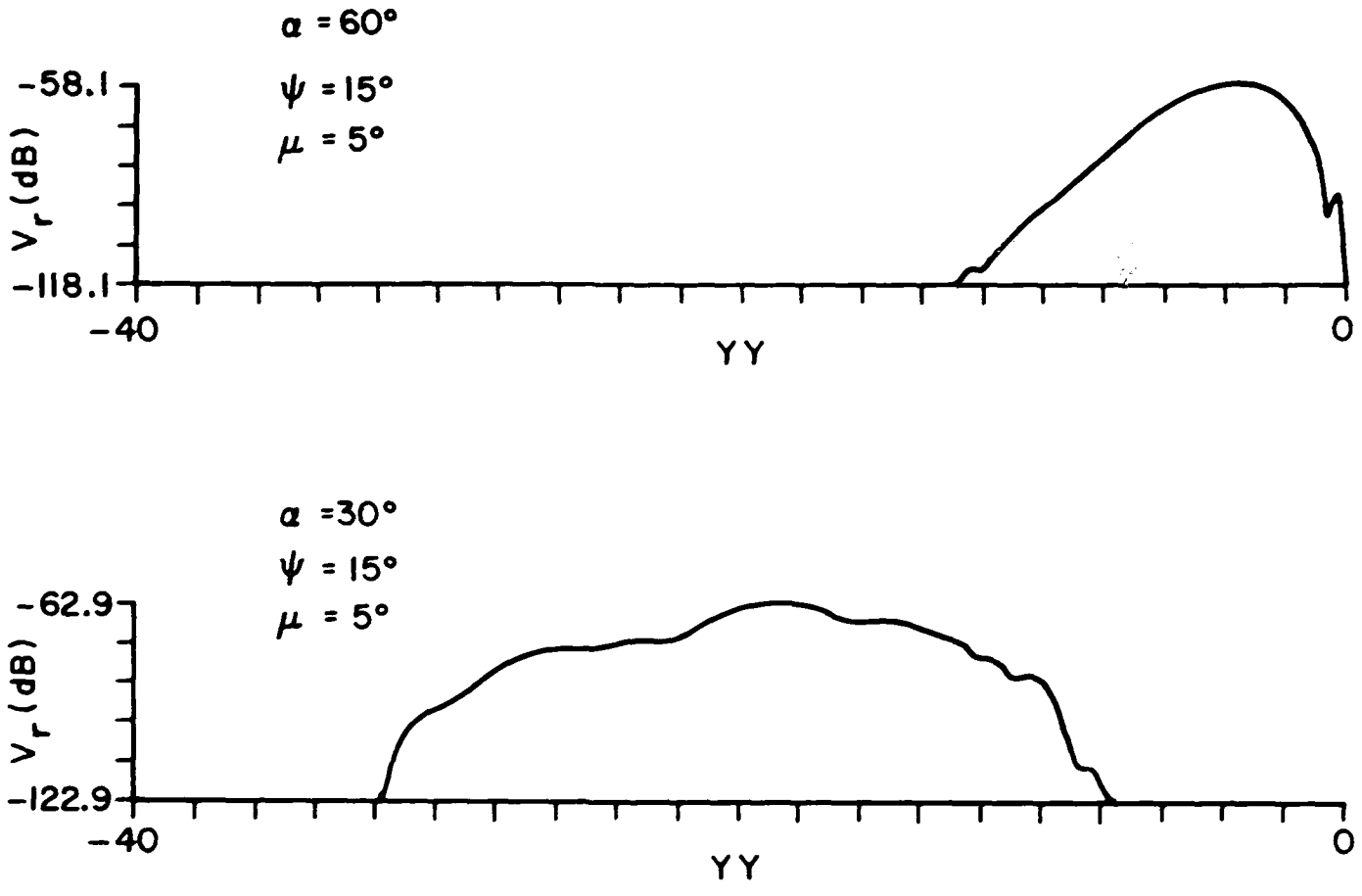

Figure 5-5b. Signatures for double-bounce scatter from a ship model.

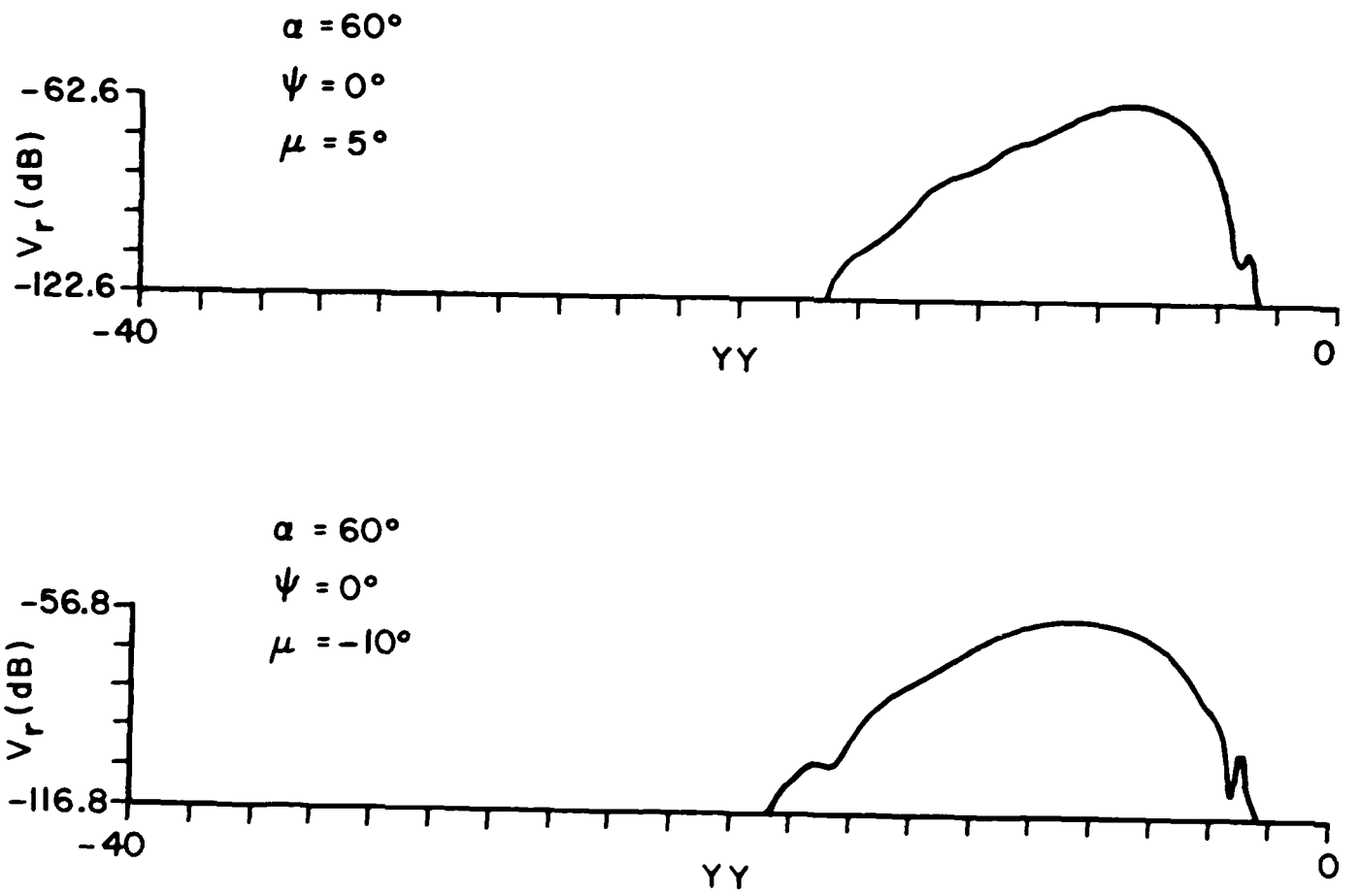

Figure 5-5c. Signatures for double-bounce scatter from a ship model.

CHAPTER VI
BACKSCATTER FROM THE PLATE EDGE

In the previous section it was found that a significant return can be expected from the double-bounce mechanism. There may also be a contribution due to diffraction from the edge of the plate. When an incident or reflected field interacts with the edge of the plate, there is a field diffracted in all directions. Because of the method of solving for the double-bounce scattering, the edge-sea surface interactions have been accounted for. Hence, the only field contribution that has not been considered is that which is diffracted directly back to the radar. The Geometrical Theory of Diffraction (GTD) is used to study this contribution.

A. Geometry

The GTD solution requires only a knowledge of the plate and radar positions; the sea surface does not affect the direct diffraction from the plate edge. As before, the radar approaches from the negative y-direction, with the distance from the radar to the plate edge defined as R_g. The geometry of the plate and radar is shown in Figure 6-1.

B. Equation for Backscatter

Since here we are only concerned with the edge diffraction, the flat plate can be considered as the limiting case of the wedge, for which much work has already been done. In reference [4] an expression is given for the diffracted field from a wedge. For receiver distances R from the edge which are approximately equal to the distance R_0 of the source from the edge, this diffracted field is given as

$$u^d = \frac{e^{-jk(R+R_0)}\, e^{jk\left(\frac{RR_0}{R+R_0}\right)}}{(R+R_0)} \left[V_B\left(\frac{RR_0}{R+R_0}\,,\ \psi'-\psi'_0\right) \pm V_B\left(\frac{RR_0}{R+R_0}\,,\ \psi'+\psi'_0\right) \right] \quad (45)$$

where the choice of sign ($\pm$) is determined by the polarization of the field. The minus sign applies for an electric field polarized parallel to the edge, and the plus sign for perpendicular to the edge. V_B is the diffraction function and is defined in Reference [4]. The angles ψ' and ψ'_0 are defined in Figure 6-1, and are equal for a monostatic radar. Similarly, the distances R and R_0 are equal and are defined in Figure 6-1 to be the distance R_g. Equation (45) then simplifies to

$$u^d = \frac{e^{-j2kR_g} e^{jkR_g/2}}{2R_g} \left[V_B(R_g/2, 0.) - V_B(R_g/2, 2\psi_o')\right] . \qquad (46)$$

Here we have chosen the minus sign since we are dealing only with horizontal polarization.

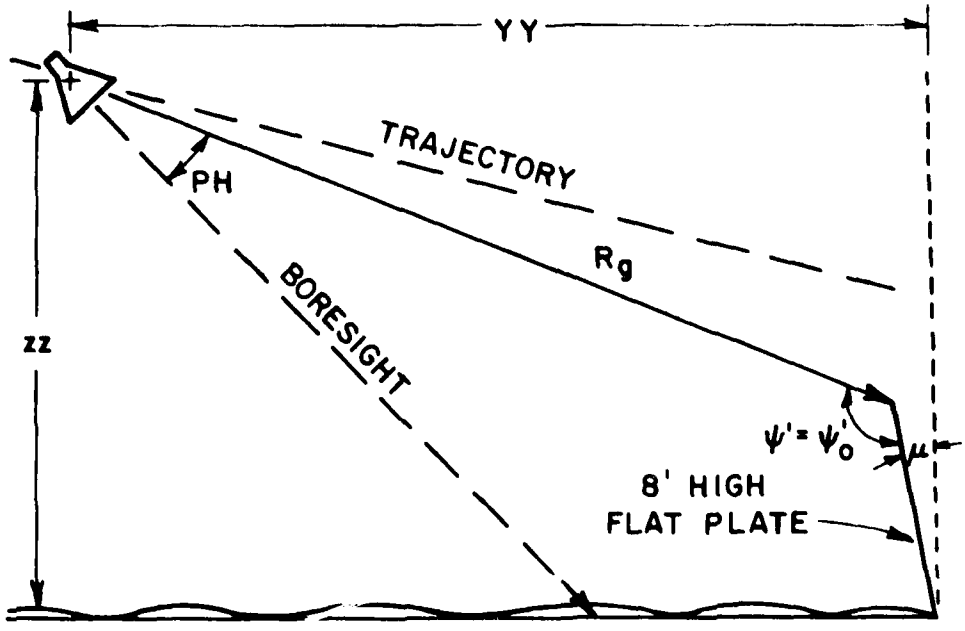

Figure 6-1. Geometry for edge diffraction.

C. Discussion of Edge Diffraction Computer Code

The calculation of the field due to diffraction from the plate edge from Equation (46) is straight forward. This calculation is made in subroutine GTDFP. The subroutine uses a computer code already available at the ElectroScience Laboratory for the computation of the diffraction function V_B. The inputs required for the subroutine are the position of the radar, and size and position of the plate. The subroutine returns the voltage at the receiver due to the diffracted

field. The calculation is made for each new position of the radar. Some diffraction signatures are shown in the following section.

D. Results for Edge Diffraction From Plate

The signatures for the field diffracted from the plate edge are shown in Figure 6-2. The model geometries that are shown for the diffraction mechanism are some of the same geometries shown for the double-bounce mechanism, Figure 5-5. Again, the range gate function $C(R_g,1)$ must be included in Equation (46).

Note that as in the double-bounce backscatter (Figure 5-5), the diffraction signatures extend over a greater range but are smaller in magnitude for near grazing incidence angles. Tilting the plate results in a shift of the position of the maximum return. Increasing the dive angle also results in a signature extended over a greater range.

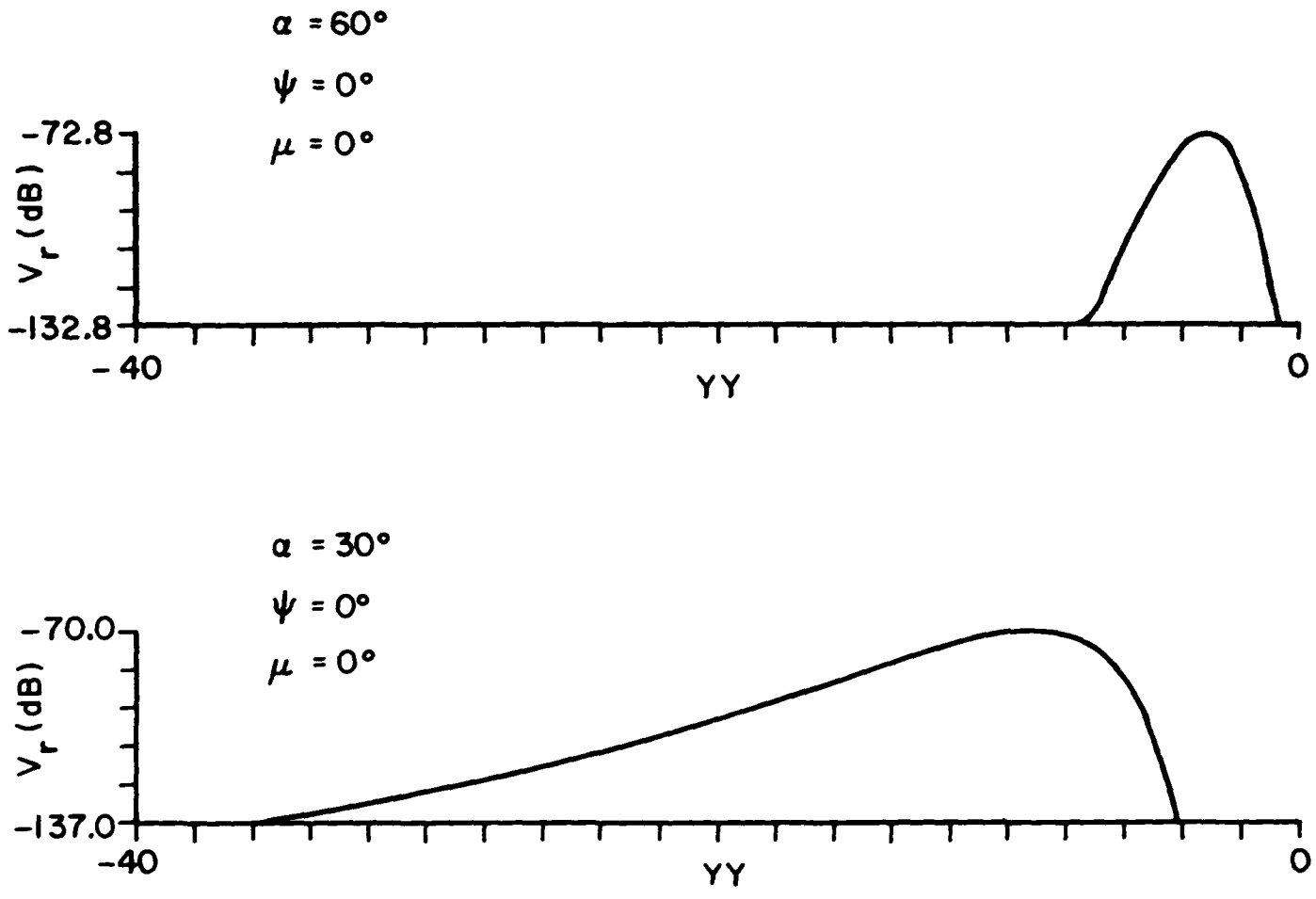

Figure 6-2a. Signatures for diffraction from plate edge.

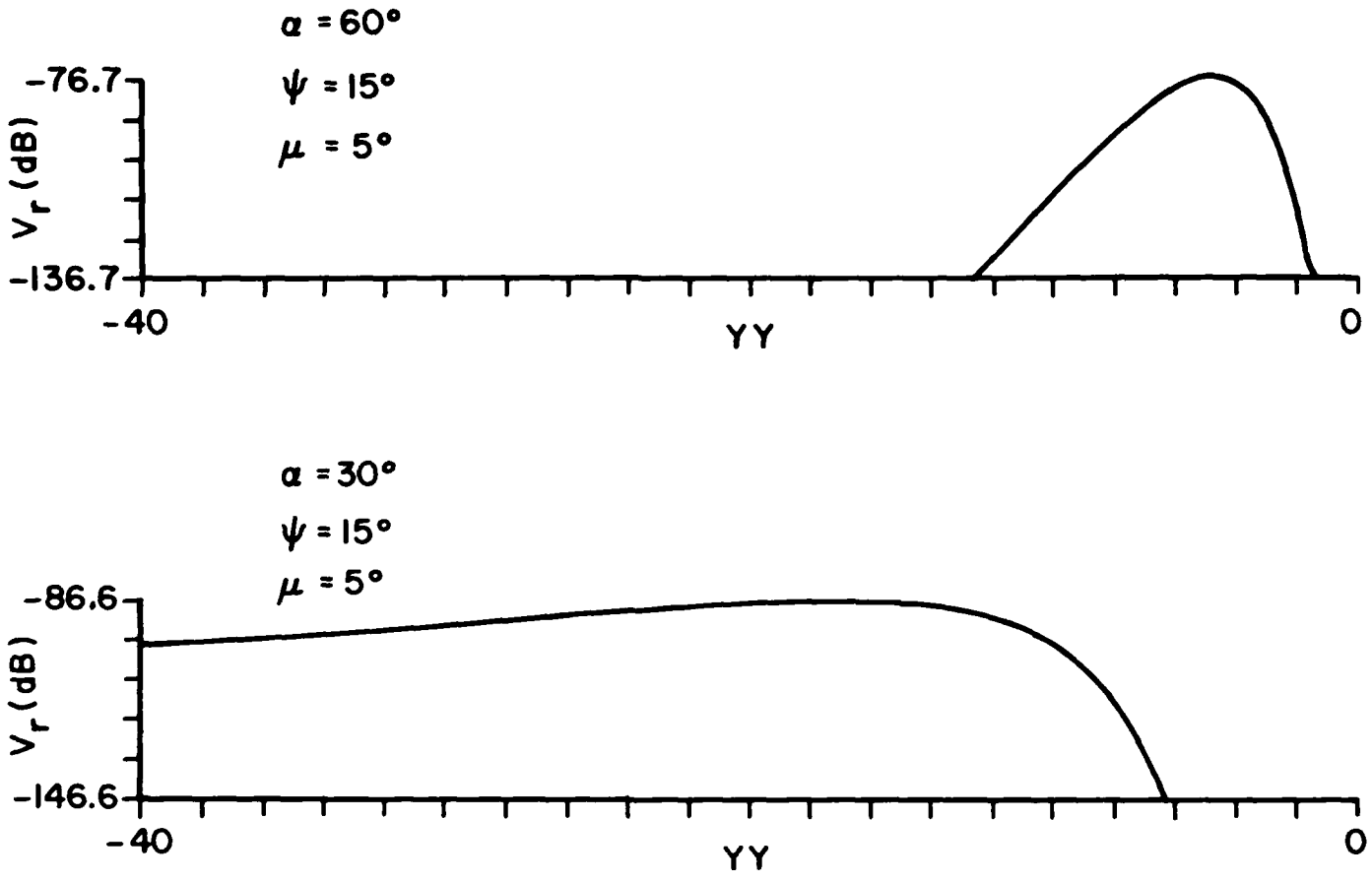

Figure 6-2b. Signatures for diffraction from plate edge.

CHAPTER VII
COMPLETE MODEL FOR SHIP-SEA SCATTERING

The previous sections illustrated the four principal mechanisms for backscattering. Each mechanism was considered independently of the others to show how each contributed to the total ship-sea backscattering problem. Since we are measuring the voltage at the receiver, superposition allows us to sum the voltages due to each of the independent scattering mechanisms. The result is the measured receiver voltage due to scattering from the complete ship-sea model (Figure 1-1).

A. Comparison with Measured Results

Figure 7-1 shows the comparison between a signature calculated by superposition, and the signature for the corresponding geometry as measured at the Encounter Simulation Laboratory. A check of the accuracy of the absolute level of the calculated receiver voltage can be obtained by using the return from a calibration sphere as a reference. The sphere return was calculated using the radar range Equation [5] for a 14" diameter sphere placed 18'7" from the trajectory of the radar. From Figure 7-1 it is clearly seen that the calculated and measured magnitudes of the scattering signatures are at the same level relative to the calibration sphere return. In all of the signatures in Figure 7-2, the level of the experimental signature relative to the calculated signature was determined by superimposing the calculated and measured sphere responses. The measured signatures are also identified by the experimental run number [3].

Figure 7-2 shows the comparison between the complete model signatures and the experimental data for a variety of model geometries. In all signatures the short range gate was used. Note that in most of the signatures the double-bounce contribution is easily identifiable as a change in the magnitude of the signature. In the geometries of Figures 7-2a through 7-2c, the contribution from edge diffraction can be seen as the last lobe on the signature. In all of the signatures the quasi-random return from the trapezoids is modulated by the gravity wave (sinusoidal) contribution in the "clutter" region of the signature.

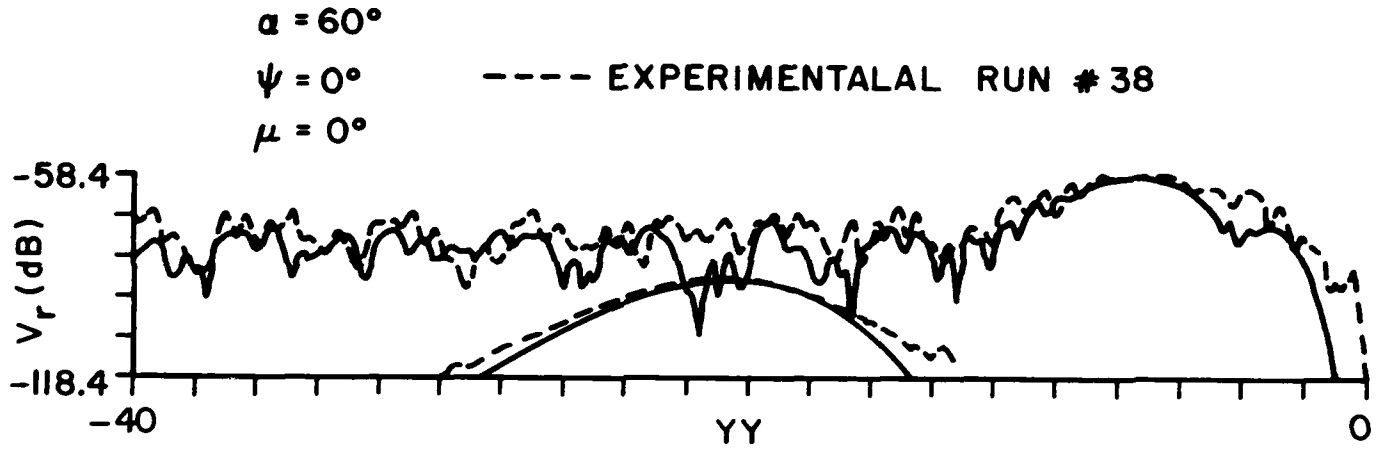

Figure 7-1. Comparison of experimental and calculated signatures showing calibration sphere response.

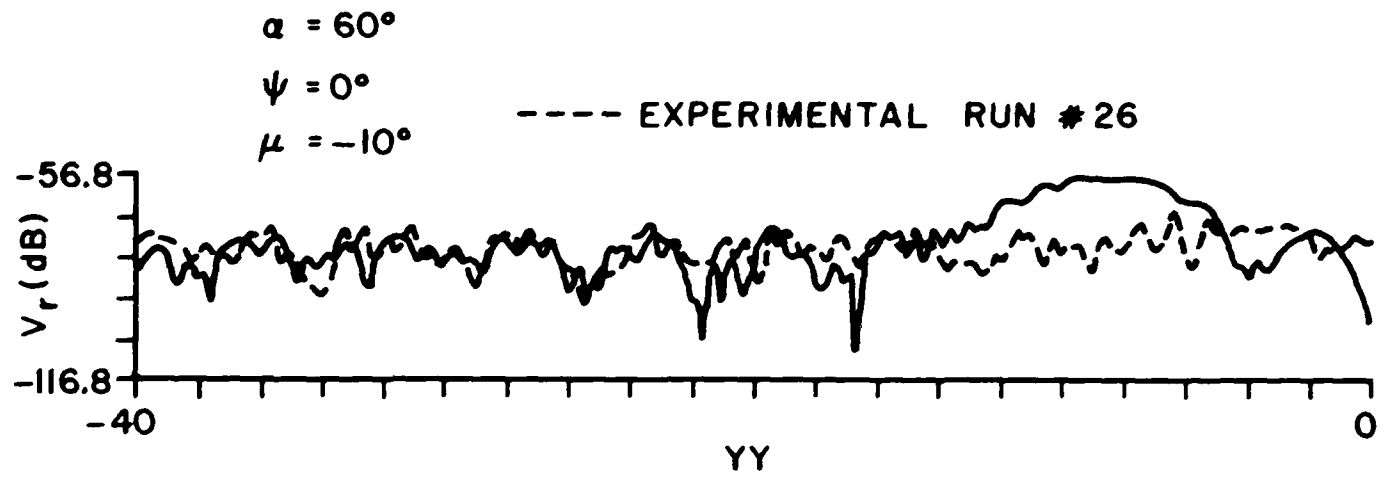

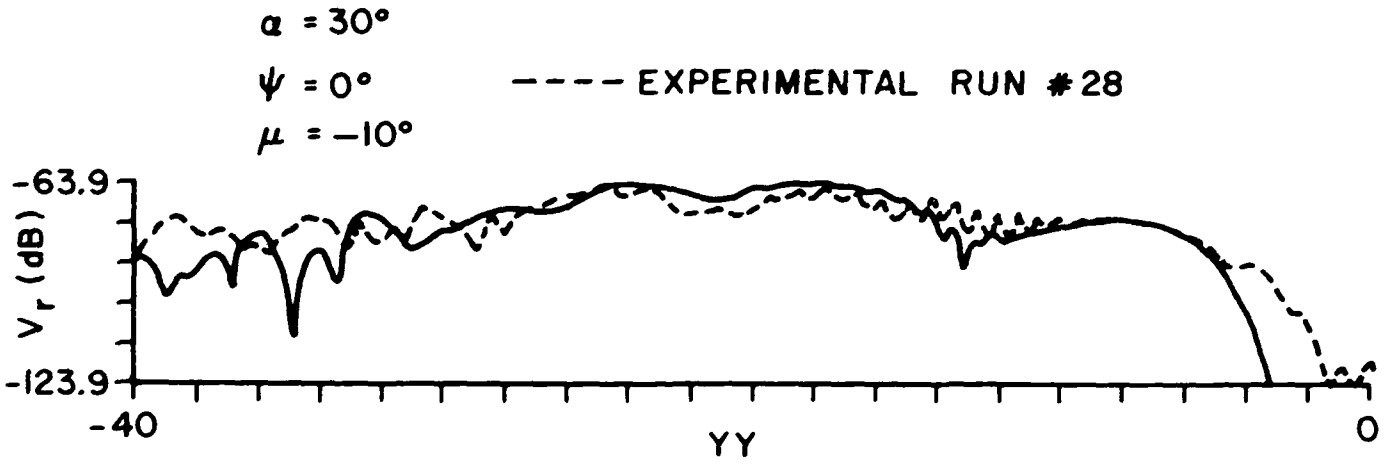

Figure 7-2a. Comparison of calculated and experimental signatures.

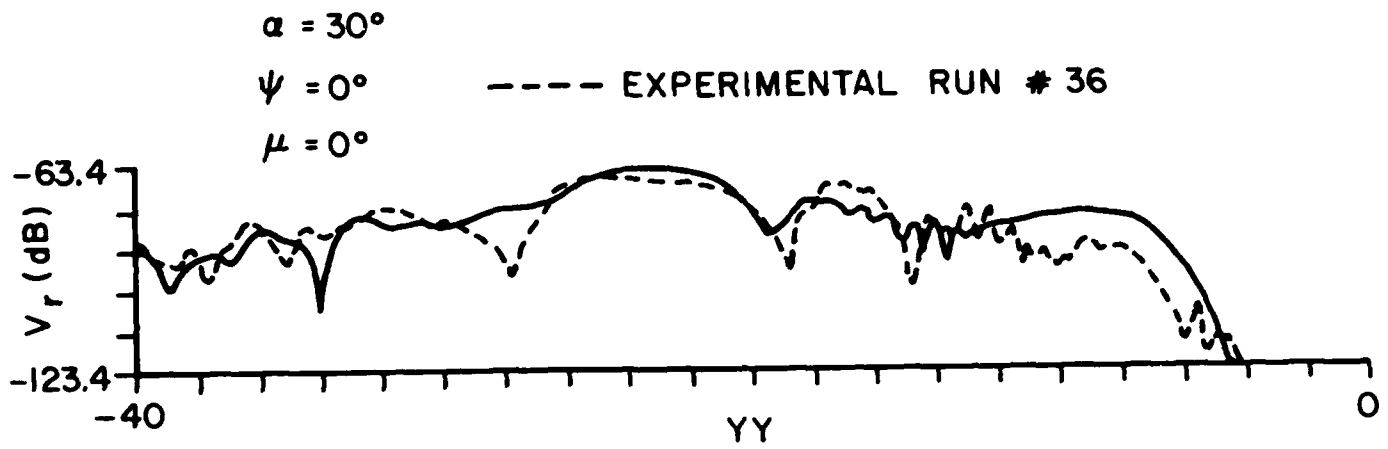

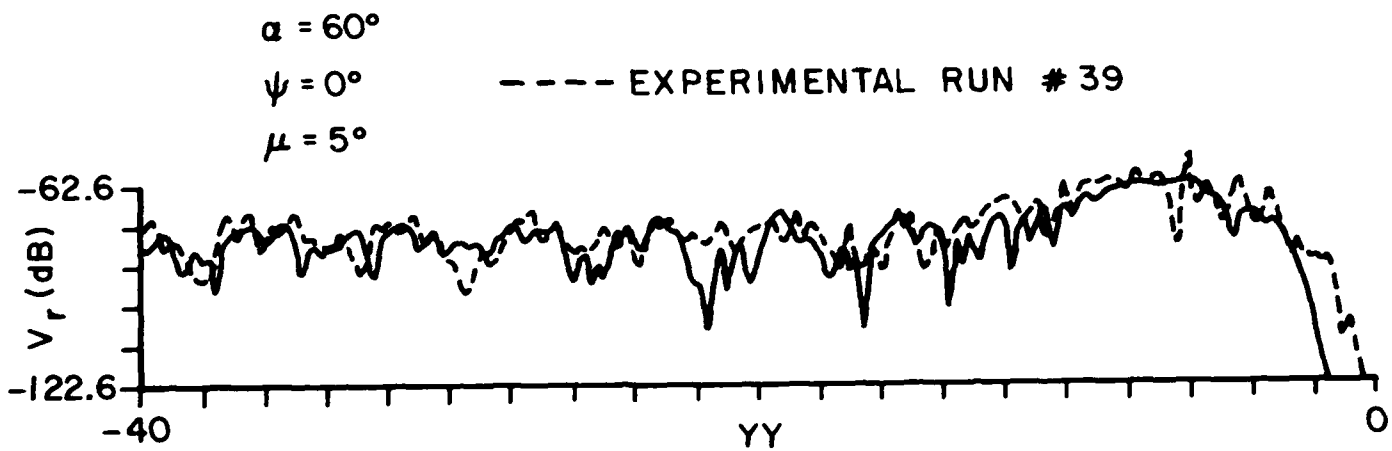

Figure 7-2b. Comparison of calculated and measured signatures.

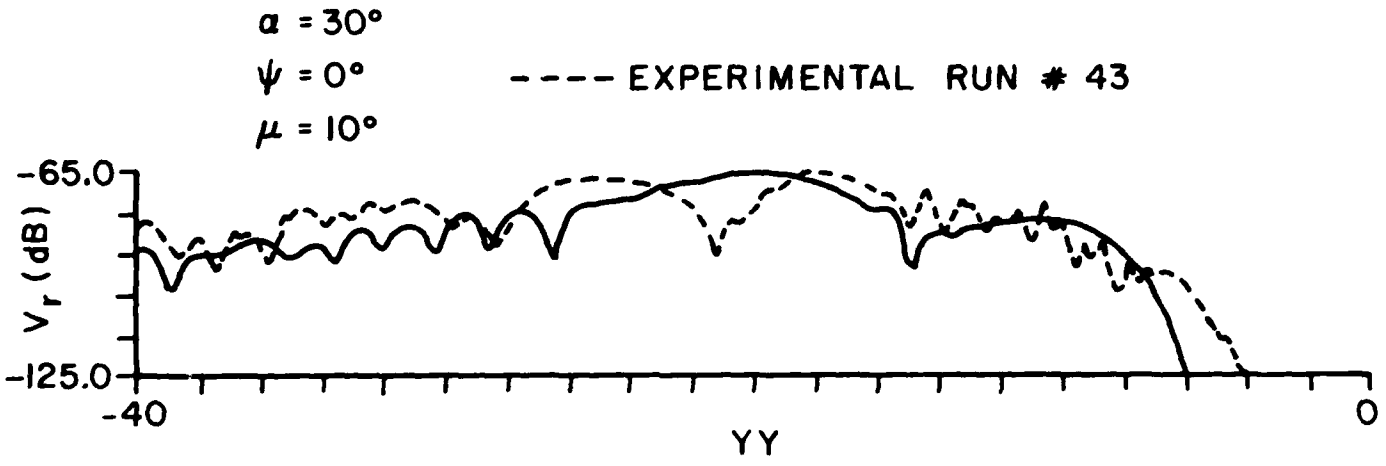

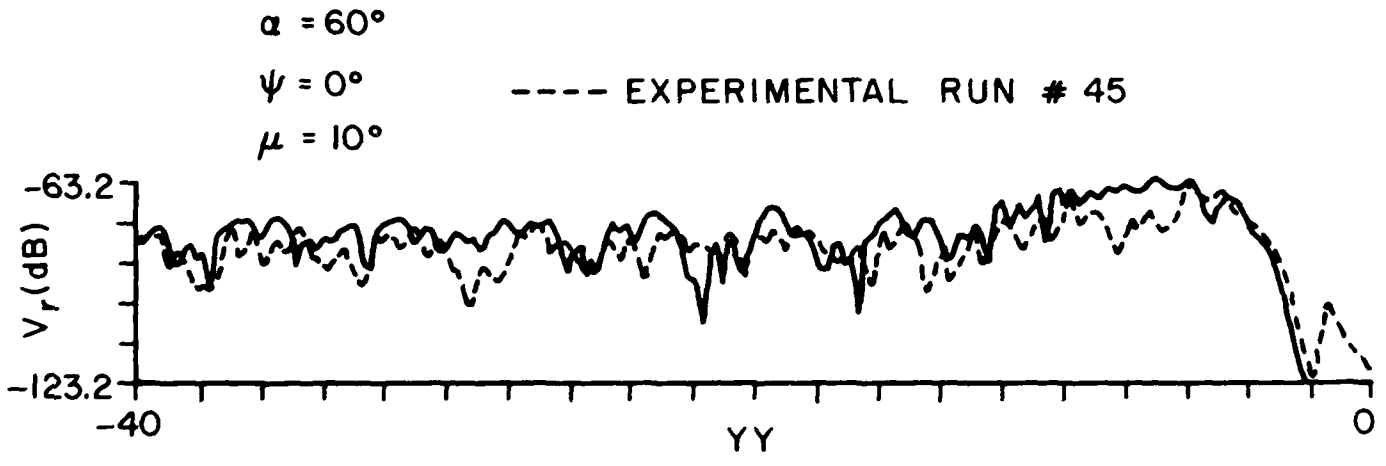

Figure 7-2c. Comparison of calculated and measured signatures.

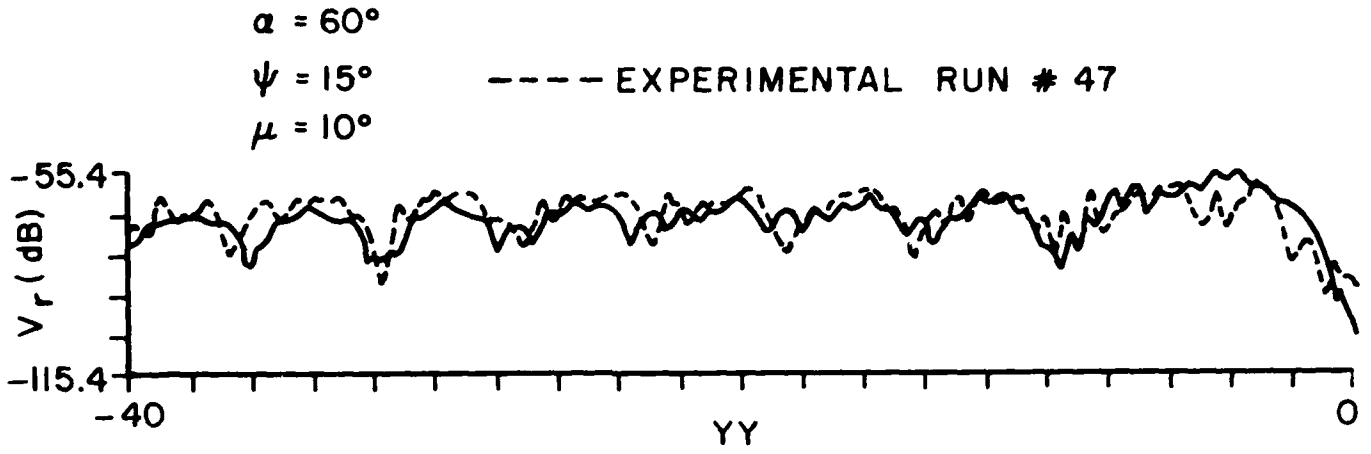

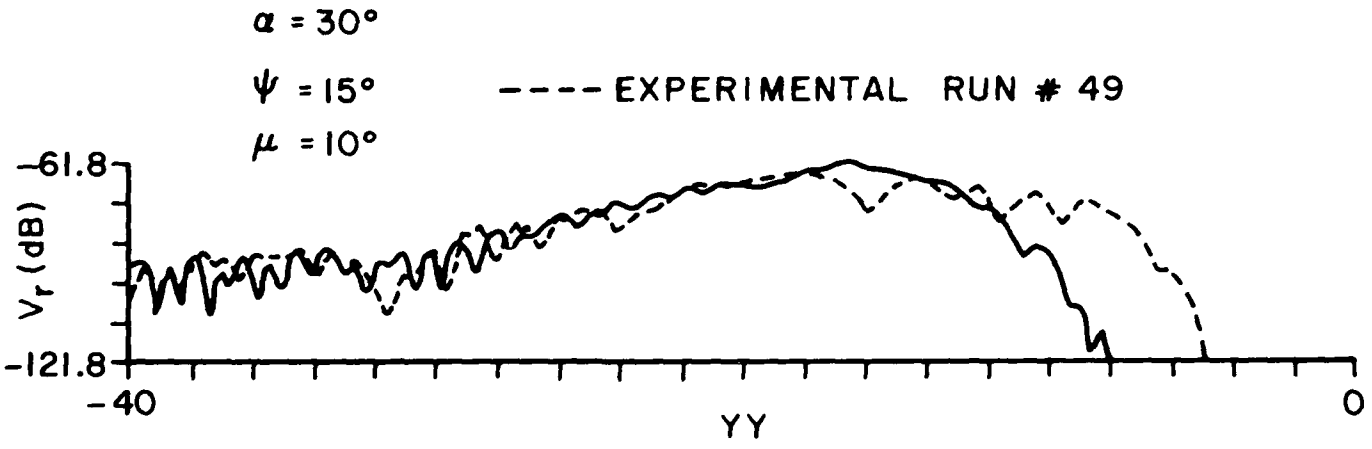

Figure 7-2d. Comparison of calculated and experimental signatures.

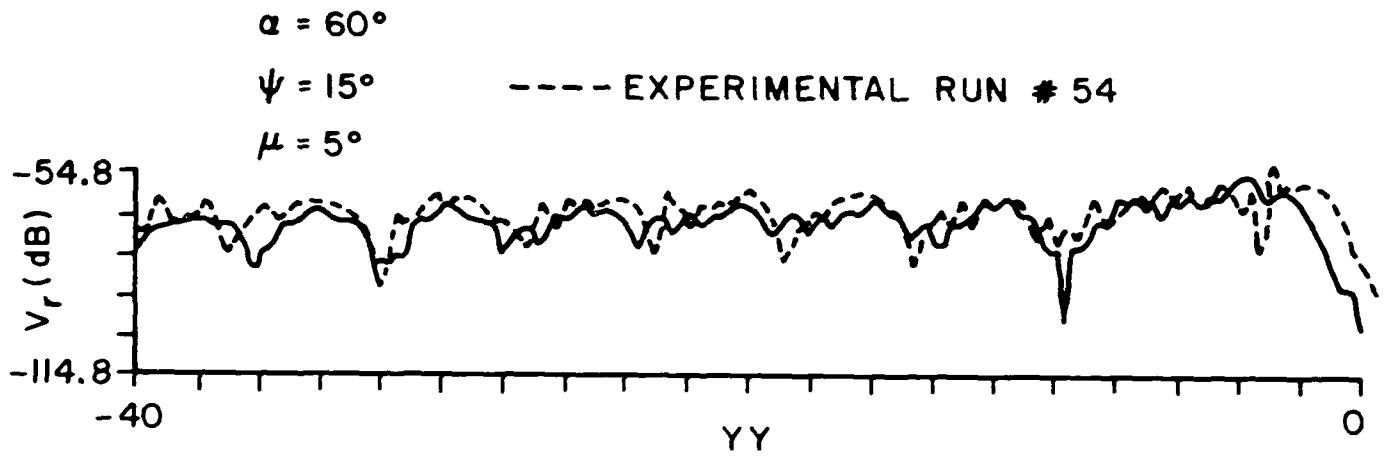

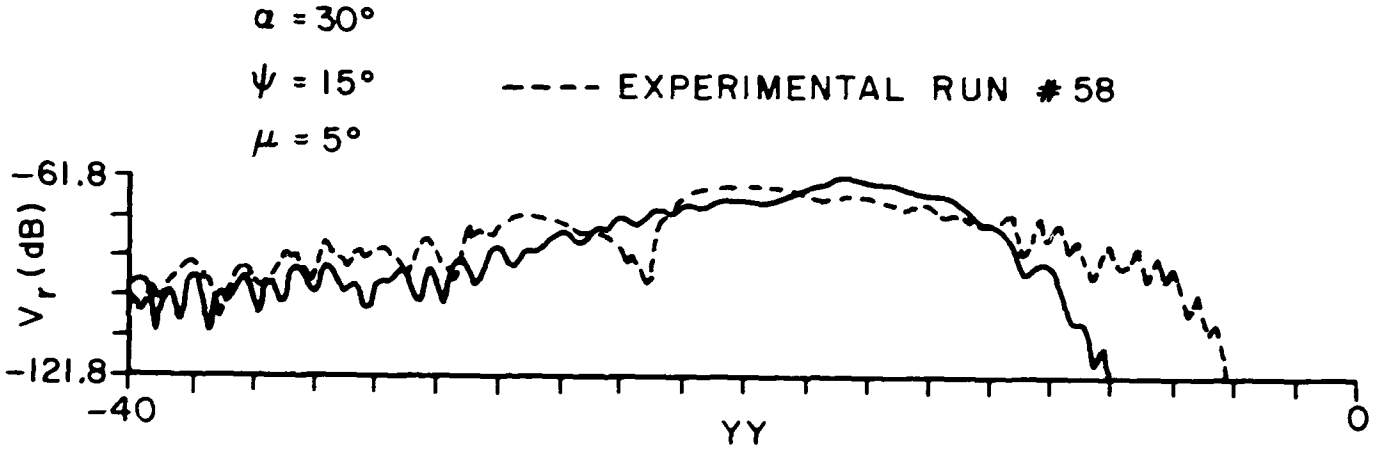

Figure 7-2e. Comparison of calculated and experimental signatures.

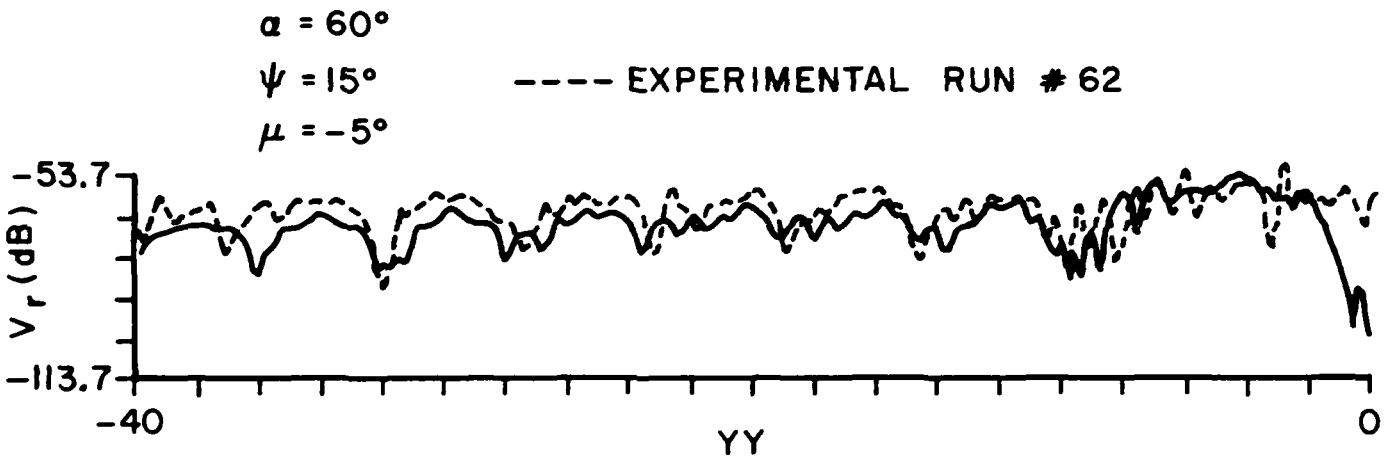

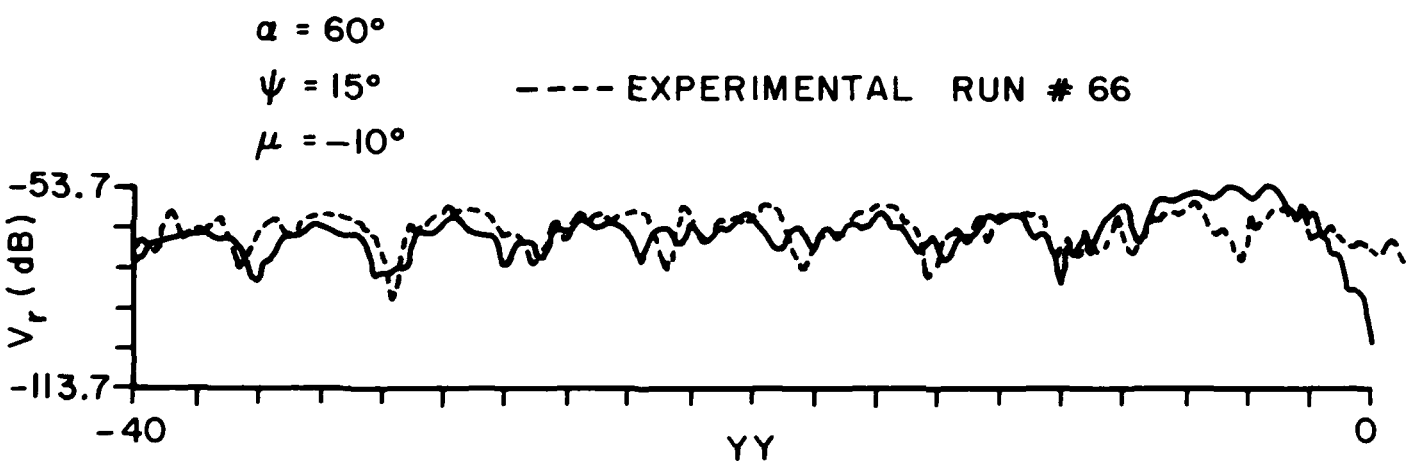

Figure 7-2f. Comparison of calculated and experimental signatures.

CHAPTER VIII
SUMMARY AND CONCLUSIONS

The purpose of this report was to develop a method for numerically calculating the backscatter from a simple one-dimensional sea-ship model. The surface was a "composite" model of the sea surface with the large scale gravity waves modeled by a sinusoid and the capillary waves modeled by trapezoids periodically superimposed on the sinusoidal surface. The ship model was composed of a metal flap mounted on the surface model.

For this ship-sea model there are four principal scattering mechanisms that contribute to the backscattered signature; namely, backscatter from the gravity waves, backscatter from the capillary waves, double-bounce scatter from the ship-sea corner, and diffraction from the edge of the plate. Since the surface model was too large to employ the more exact moment method, the first three of these mechanisms were analyzed using the physical optics approximation, while the last mechanism was calculated by a direct application of the Geometrical Theory of Diffraction. The voltage received at the antenna terminals was calculated for each of the scattering mechanisms.

The results were presented in a form showing the contribution from each of the individual scattering mechanisms, and these were then combined to produce the total received voltage as a function of radar position. The resulting signatures compared favorably with the measured data from the Naval Weapons Center, both in absolute level and in the spatial variation of the signature.

Thus, the technique presented here provides an accurate and efficient method of determining the backscatter from simple one-dimensional ship-sea models. The accuracy of the results were limited mainly by the use of the physical optics approximations. The running time of the one-dimensional surface programs could be reduced by employing a faster integration scheme, since no special effort was made to produce an efficient computer code.

It should also be noted that the physical optics technique can be applied to a wide variety of surface structures and experimental configurations provided the integration increments are properly chosen. For example, the antenna power pattern or polarization of the radar system can be easily changed from those used in this study. The ability to separate the contributions of the four scattering mechanisms, and to associate a range and doppler shift with each point on the surface, provides a convenient method for investigating the effects of a variety of range gates, doppler filters, polarizations, etc. on system performance.

APPENDIX
COMPUTER CODE SSSCAT

A listing of the computer code discussed in the text is presented here. To facilitate the understanding of the code, the symbols used in the program have been used in the text whenever possible. Note that the code may employ programming features not universal to all computer systems.

```
C     PROGRAM SSSCAT *** BY DAN RYAN
C     PROGRAM CALCULATES THE FIELD SCATTERED FROM A
C     SHIP-SEA MODEL FOR A HORIZONTALLY POLARIZED INCIDENT
C     FIELD.  THE MODEL IS COMPOSED OF A FLAT PLATE MOUNTED
C     ON A SINUSOIDAL SURFACE.
C     THE MAIN PROGRAM CALCULATES THE FIELD SCATTERED
C     FROM THE GRAVITY WAVE MODEL.  SUBROUTINE SPPS CALCULATES
C     THE FIELD SCATTERED FROM THE CAPILLARY WAVE MODEL.
C     SUBROUTINE DBSGTD CALCULATES THE DOUBLE BOUNCE
C     SCATTER FROM THE CORNER CREATED BY THE SURFACE AND PLATE.
C     DBSGTD CALLS SUBROUTINE GTDFP WHICH CALCULATES
C     THE DIFFRACTED FIELD FROM THE PLATE EDGE.
C     *****
C     SSSOUT = OUTPUT FILE WHERE DATA IS STORED
C     ALPHA  = ANGLE BORESIGHT MAKES WITH TRAJECTORY(DEG)
C     PHID   = TRAJECTORY ANGLE MEASURED FROM HORIZONTAL(DEG)
C     MU     = ANGLE PLATE MAKES WITH VERTICAL(DEG)
C     THETA  = ANGLE BORESIGHT MAKES WITH VERTICAL(DEG)
C     HEII   = PEAK AMPLITUDE OF SURFACE(FT)
C     HP     = HEIGHT OF PLATE(FT)
C     D1     = ALTITUDE OF RADAR ABOVE SURFACE AT YS=0.(FT)
C     BWH    = HORIZONTAL 3DB BEAMWIDTH(DEG)
C     BWV    = VERTICAL 3DB BEAMWIDTH(DEG)
C     PHASE  = PHASE SHIFT OF SINUSOIDAL SURFACE(DEG)
C     EL     = ELECTRICAL WAVELENGTH(FT)
C     KP     = ELECTRICAL WAVE NUMBER
C     WM     = MECHANICAL WAVE NUMBER
C     VXYY   = COMPLEX VOLTAGE AT RADAR DUE TO FIELD SCATTERED
C              FROM SEA-SHIP MODEL(VOLTS)
C     DT     = DISTANCE ALONG TRAJECTORY(FT)
C     TM2    = STARTING POINT OF RADAR
C     DTM2   = INCREMENT ALONG TRAJECTORY(FT)
C     *****
C
C
      INCLUDE MESSB,SYS9
      DIMENSION VXYY(200),DT(200)
      COMMON/PIS/PI,TPI,DPR
      COMMON/FUNF/YY,ZZ,YO,RO
      COMMON/ANG/THETA,THI,PHID,PHT,ALPHA,ALP,MU,MUR
      COMMON/SURF/PHASE,HEII,HP,DC,WM
      COMMON/ANT/BWV,BWH,A,B,EL,VC,M,KP
      COMPLEX DEN2,DEN1,PEP
      COMPLEX PEP1,X1,VX,VXT,VSTP
      COMPLEX VXYY,VOBS
      REAL DT,KP,MU,MUR
      CALL GETCF('CO)
      CALL ASSIGN(6HSSSOUT,5H3266P,1)
      CALL ASSIGN(4H$MSG,0.,3)
      HEII = .146
      HEI = HEII
      HP = 3.0
      DO = 3.03125
      BWH = 15.0
      BWV = 15.0
```

```
      PHASE = 10.
      FL =
      WM = 4.99736*.3048
      KP = 2.*PI/EL
      P = .6931472/(TAN(BWH/114.591)**2
      P = .6931472/(TAN(BWV/114.591)**2
      CALL SUPERR(3)
      VO = 1.0
      WRITE(6,10)
      READ(5,*)D1
   10 FORMAT(' TYPE D1=?   ')
      WRITE(6,11)
      READ(5,*)ALPHA,PHID,MU
   11 FORMAT(' TYPE ANGLES ALPHA; PHID; MU=?  ')
      WRITE(6,13)
      READ(5,*)M
   13 FORMAT(' TYPE 1/2,LONG/SHORT; M=?  ')
      CALL DEASSN
      THETA = 90.-ALPHA-PHID
      THI = THETA/DPR
      PHI = PHID/DPR
      ALP = ALPHA/DPR
      MUR = MU/DPR
      TM2 = 39.4167/COS(PHI)
      DTM2 = TM2/200.
      DD = (D1-D0)/COS(PHI)
      KKK = 200
      DO 41 N = 1,KKK
      WRITE(3,111)N
  111 FORMAT(' PROGRAM IS IN N=',I3,' LOOP')
      CLOSE 3
      XT(N) = N-1
      TM2 = TM2-DTM2
      DDP = TM2*SIN(PHI)
      ZZ = DD*COS(PHI)
      YY = TM2*COS(PHI)
      BTA = PI/2.+THI
C
C     THE FOLLOWING SETS UP THE BOUNDARIES OF INTEGRATION
C     AS DEFINED BY THE BEAMWIDTH.
C
      RO = ZZ/SIN(PI/2.-THI)
      RRO = RO
      RRO = RO**2
      RRRO = RRO**2
      CTH = COS(THI)
      STH = SIN(THI)
      XO = ZZ
      YO = -RO*STH
      YPOS = YY+YO
      YS1 = YO+HO*TAN(THI-1.5*BWV/DPR)
      P1 = THI+1.5*BWV/DPR
      IF(P1.GT.1.55)P1=1.55
      YS2 = YO+HO*TAN(P1)
      YS18 = YS1-YO
```

```
      IF(YS2.GT.YPOS)YS2=YPOS
C
C
C     THIS SECTION INTEGRATES OVER THE ANTENNA FOOTPRINT.
C     THE RESULT IS THE VOLTAGE RECEIVED BACK AT THE
C     POINT OF TRANSMISSION. (VOLTS)
C
C
      VXY = (0.0,0.0)
      IF(YS1.GE.YY)GO TO 51
      DY = 0.01
      Y = YS1
   31 YS = -Y0-YY+Y
      HEI = HEII
      IF(YS.GE.-.08333)HEI=0.
      H = HEI+HEI*SIN(WM*YS+PHASE*PI/180.)
      YR = YS+.005
      HR = HEI*SIN(WM*YR+PHASE*PI/180.)
      R2 = R0+Y*STH-H*CTH
      RR2 = R2**2
      RR1 = (Y-Y0)**2+(H-H0)**2
      R1 = SQRT(RR1)
      RRP1 = RR1
      RP1 = SQRT(RRP1)
      TNE = (Y*CTH+H*STH)/R2
      TNE2 = TNE**2
      RP2 = RP0-Y*COS(BTA)-H*SIN(BTA)
      RRP2 = RP2**2
      TNEP = H*COS(BTA)/RP2-Y*SIN(BTA)/RP2
      IF(TNEP.GT.1.5)TNEP=1.5
      TNEP2 = TNEP**2
      IF(TNEP2.GT.2.)TNEP2=2.
      T = -RP*(R1*RRP1*RR2*RRP2+RR2*RRP2*RR1*RP1)
      S = -(A*RR1*RRP1*RRP2+RR2*RRP1*RPP2+3.*RR1*RR2*RRP2)
      S = S-A*RR1*RRP1*RP2
      CEN2 = CMPLX(S,T)
      CEN1 = CSQRT(CEN2)
      PE = -RP*(R1+RP1)+PI/2.
      REO = 0.0
      PEP = CMPLX(REO,PE)
      PEP1 = CEXP(PEP)
      X1 = RO*R2**2.*RP2*PEP1/CEN1
      PH = ATAN(WM*HEI*COS(WM*YS+PHASE*PI/180.))
      AJ1 = CTH*STH*TAN(PH)+Y/RO*TAN(PH)-H/RO
      ABE = AB1/R1
      CLEO = EXP(-H/2.*TNE2)
      CLEOP = EXP(-H/2.*TNEP2)
      CLEOP = CLEO
      R = (R1+RP1)/2.
      VX = -1.*X1*DY*ABE*CLEO*CLEOP*V0*C(R,*)/SQRT(PI*R.)
      VXY = VXY+VX
      Y = Y+DY
      IF(Y.LE.YS2) GO TO 31
      DO 81 JJ=1,N0
      DO 81 K=1,2
```

```
      YM=-JJ*0.66667+0.125
      IF(K.EQ.2)YM=YM-0.14567
      CALL SPRS(VSTP,YM,TN1)
      VXY=VXY+VSTP
   81 CONTINUE
   51 CALL DRSGTO(VOBS,YY,ZZ)
      VXYY(N) = VXY+VOBS
   41 CONTINUE
      WRITE(1) (VXYY(N),N=1,KKK)
      CALL GETCP(NCP)
      CP = (NCP-NCO)/100.
      WRITE(3,600)CP
  600 FORMAT('0',10X,'TOTAL CPU=',F8.2)
      CALL EXIT
      END
C
C
      BLOCK DATA
      LOGICAL LTEST,LDEBUG
      DIMENSION P(5),L(5)
      REAL L
      COMMON/TEST/LTEST,LDEBUG
      COMMON/PIS/PI,TPI,DPR
      COMMON/PTS/P,L
      DATA PI,TPI,DPR/3.1419265,6.2831531,57.29577950/
      DATA LTEST,LDEBUG/.FALSE.,.FALSE./
      DATA P/0.04069,0.038460,0.04069,0.026,0.026/
      DATA L/-1.0,-1.0,1.0,-1.0,-1.0/
      END
C
C
C
C     RANGE GATE.
      FUNCTION C(R,M)
C
C
C
C
C
C
C
C
C
C
C
   4  CONTINUE
      RETURN
      END
C
C
C     SUBROUTINE SPRS CALCULATES THE SCATTERING
C     FROM THE SMALL TRAPEZOIDAL PERTURBATIONS
C     THIS IS A BRAGG SCATTER CONTRIBUTION
C
C
```

```
      SUBROUTINE SPHS(VSTP,YM,THI)
      DIMENSION P(5),L(5),HS(5),YP(5),DWY(5),SIG(5)
      COMMON/SURF/PHASE,HEII,HP,DD,AM
      COMMON/ANT/RHV,BHH,A,B,FL,VO,M,KP
      COMMON/PIS/PI,TPI,DPR
      COMMON/FUNF/YY,ZZ,YJ,RO
      COMMON/PTS/P,L
      COMPLEX J,VSTP,DEN2,DEN1,VS,ARG,CARG
      REAL L,KP,NU
      J=(0.,1.0)
      NU=ATAN(.55563/1.10877)
      RHO=49.3496/DPR
      STH = SIN(THI)
      CTH = COS(THI)
      YS=YM
      HEI = HEII
      IF(YS.GE.-.70833)HEI=0.
      HE=HEI+HEI*SIN(WM*YS+PHASE*PI/180.)
      ZZ=ZZ
      DH=WM*HEI*COS(WM*YS+PHASE*PI/180.)
      EPS=ATAN(DH)
C
C
C     THE FOLLOWING DEFINES THE GEOMETRY OF THE
C     TRAPEZOIDS.  HS AND YP DEFINE THE POSITION OF THE
C     CURRENT ELEMENT IN EACH SEGMENT.
C
C
      HS(1)=P(1)*SIN(NU-EPS)
      HS(2)=P(2)*COS(EPS)
      HS(3)=P(3)*SIN(NU+EPS)
      HS(4)=P(4)*SIN(-EPS)
      HS(5)=P(5)*SIN(-EPS)
C
      YP(1)=-P(1)*COS(NU-EPS)
      YP(2)=-P(2)*SIN(EPS)
      YP(3)=P(3)*COS(NU+EPS)
      YP(4)=P(4)*COS(EPS)
      YP(5)=-P(5)*COS(EPS)
C
      SIG(1)=RHO+EPS
      SIG(2)=EPS
      SIG(3)=RHO-EPS
      SIG(4)=EPS
      SIG(5)=EPS
C
      DWY(1)=.048*COS(RHO+EPS)
      DWY(2)=.041*COS(EPS)
      DWY(3)=.048*COS(RHO-EPS)
      DWY(4)=.152*COS(EPS)
      DWY(5)=.152*COS(EPS)
C
C     THIS SECTION CALCULATES THE VOLTAGE AT THE
C     RECEIVER DUE TO THE FIELD SCATTERED FROM
C     EACH SEGMENT OF THE TRAPEZOID. (VOLTS)
```

```
C
      VSTP=(0.,0.)
      DO 70 N=1,5
      HH=HS(N)+H
      YT=YO+YY+YM+YP(N)
      R2=RO+YT*STH-HH*CTH
      RR2=R2**2
      RR1=(YT-Y0)**2+(HH-H0)**2
      R1=SQRT(RR1)
      TN=(YT*CTH+HH*STH)/R2
      TNT=TN**2
      IF(TNT.GE.2.)TNT=2.
      S=2./RR1+A/RR2
      T=KP/R1
      DEN2=CMPLX(S,T)
      DEN1=CSQRT(DEN2)
      REC=EXP(SIG(N))*(YT+RC*STH)*COS(SIG(N))*(HH-RO*CTH)
      BLUE=(HH-RO*CTH)**2+(YT+RO*STH)**2
      BLUE=COS(SIG(N))*SQRT(BLUE)
      CLEO=EXP(-B*TNT)
      ARR=-2.*J*KP*R1
      CARR=CEXP(ARR)
      VS=-VO*J*REC/BLUE*DWY(N)*CLEO*CARR/DEN1/2./RR1/SQRT(PI)
      VS=VS*C(N1,N)
      IF(N.GE.N)VS=-VS
      VSTP=VSTP+VS
   70 CONTINUE
      RETURN
      END
C
C
C
C
C     THIS SUBROUTINE CALCULATES THE DOUBLE BOUNCE
C     SCATTER FROM A FLAT PLATE AT A SPECIFIED ANGLE TO A
C     COMPOSITE SINUSOIDAL SURFACE.  THE SOLUTION ALSO
C     CONTAINS THE EDGE DIFFRACTION FROM THE TIP OF
C     THE PLATE.  THE FIELD IS HORIZONTALLY POLARIZED.
C
C
      SUBROUTINE OBSGTD(VOBS,YY,ZZ)
      COMMON/ANG/THETA,THI,PHID,PHI,ALPHA,ALP,MU,MUR
      COMMON/SURF/PHASE,HEII,HP,DD,NN
      COMMON/ANT/BWV,BWH,A,B,EL,VO,M,KP
      COMPLEX DEN2,DEN1,PEP
      COMPLEX PEP1,X1,VX,VXY,VOBS
      COMMON/PIS/PI,TPI,DPR
      COMPLEX EXYY,DD
      REAL KP,MU,MUR
      HEI = HEII
      RTA = PI/2.-THI*2.*MUR
C
C     THE FOLLOWING SETS UP THE BOUNDARIES OF INTEGRATION
C     AS DEFINED BY THE BEAMWIDTH.
C
```

```
      YNEG = -HP*YY/(ZZ-HP)
      YO = -RO*SIN(THI)
      RO = ZZ/SIN(PI/2.-THI)
      BT = PI/2.-2.*MUR+THI
      ARP = (YY+YO)*SIN(2.*MUR)/SIN(BT)
      RPO = RO+ARP
      RRO = RO**2
      RRPO = RPO**2
      CTH = COS(THI)
      STH = SIN(THI)
      HO = ZZ
      YO = -RO*STH
      YPOS = YY+YO
      YS1 = YO+HO*TAN(THI-1.3*BWV/2PR)
      P1 = THI+1.3*BWV/2PR
      IF(P1.GT.1.55)P1=1.55
      YS2 = YO+HO*TAN(P1)
      YS1B=YPOS+YNEG
      YS2B=YPOS
      IF(YS1B.GT.YS1)YS1=YS1B
      IF(YS2.GT.YS2B)YS2=YS2B
C
C
C     THIS SECTION INTEGRATES OVER THE ANTENNA FOOTPRINT.
C     THE RESULT IS THE VOLTAGE RECEIVED BACK AT THE
C     POINT OF TRANSMISSION.  (VOLTS)
C
      SXY = (0.0,0.0)
      IF(YS1.GT.YS2)GO TO 51
      DY = 0.01
      Y = YS1
   51 YS = -YO-YY+Y
      HEI = HEII
      IF(YS.GE.-.05335)HEI=0.
      H = HEI+HEI*SIN(WN*YS+PHASE*PI/180.)
      YA = YS+.005
      HA = HEI+HEI*SIN(WN*YA+PHASE*PI/180.)
      R2 = RO+Y*STH-HO*CTH
      RR2 = R2**2
      RR1 = (Y-YO)**2+(H-HO)**2
      R1 = SQRT(RR1)
      CAT = YPOS/SIN(BT)*SIN(BTA)
      RRP1 = (YY+CAT-Y)**2+(H-RPO*SIN(BTA))**2
      RP1 = SQRT(RRP1)
      THE = (Y*CTH+H*STH)/R2
      THE2 = THE**2
      RP2 = RRO-(-2.*YY-2.*YO+Y)*COS(BTA)-H*SIN(BTA)
      RRP2 = RP2**2
      THEP = H*COS(BTA)/RP2-(-2.*YY-2.*YO+Y)*SIN(BTA)/RP2
      IF(THEP.GT.1.5)THEP=1.5
      THEP2 = THEP**2
      IF(THEP2.GT.2.)THEP2=2.
      A = -RP*(R1*RRP1*RR2*RRP2+RR2*RRP2*RP1*RP1)
      S = -(A*RR1*RRP1*RRP2+RR2*RRP1*RRP2+3.*RR1*RR2*RRP2)
      S = S-A*RR1*RRP1*RP2
```

```
      DEN2 = CMPLX(S,T)
      DEN1 = CSQRT(DEN2)
      RL = -KP*(R1+RP1)+PI/2.
      REO = 0.0
      PEP = CMPLX(REO,RL)
      PEP1 = CEXP(PEP)
      X1 = RO*R2**2.*RP2*PEP1/DEN1
      PH = ATAN(W*HEI*COS(WM*YS+PHASE*PI/180.))
      AB1 = CTH*STH*TAN(PH)+Y/RO*TAN(PH)-H/RO
      ABE = AB1/R1
      CLEO = EXP(-B/2.*TNE2)
      CLEOP = EXP(-B/2.*TNEP2)
      P = (R1+RP1)/2.
      VX = 2.*X1*DY*ABE*CLEO*CLEOP*VO*C(R,M)/SQRT(PI*8.)
      VXY = VXY+VX
      Y = Y+DY
      IF(Y.LE.YS2) GO TO 31
   51 CALL GTOFP(UO,ALP,MUR,YY,ZZ)
      VURS = VXY+UO
      RETURN
      END
C
C
C
C     SUBROUTINE GTOFP
C     SUBROUTINE CALCULATES THE CONTRIBUTION OF EDGE
C     DIFFRACTION FROM A PLATE BY MEANS OF THE
C     GEOMETRICAL THEORY OF DIFFRACTION.
C     GTOFP REQUIRES THE POSITION OF THE PLATE AND RADAR
C     AS INPUT WITH OUTPUT BEING UO, THE DIFFRACTED FIELD.
C     SUBROUTINE VB IS USED TO CALCULATE THE DIFFRACTION
C     FUNCTION.
C
C
      SUBROUTINE GTOFP(UO,ALP,MUR,YY,ZZ)
      COMMON/SURF/PHASE,HEII,HP,UO,WM
      COMMON/ANT/BWV,BWH,A,B,EL,EO,M,KP
      COMPLEX CEFG,EINC,CSMO,VB1,VB2
      COMPLEX UOA,VBC,CAP
      COMPLEX J,ARG,VBC1,VBC2,UU
      REAL MU,MUR,KP
      J = (0.,1.)
      PN = 2.
      HOR = YY-HP*SIN(MUR)
      VER = ZZ-HP*COS(MUR)
      PHO = PI(1.0)+MUR-ATAN(HOR/VER)
      RG = HOR/SIN(PI(1.0)+MUR-PHO)
      PH = ALP-ATAN(VER/HOR)
      PHOD = PHO*57.296
      ANTF = EXP(-A*(TAN(PH))**2)
      ARG = J*KP*(RG/2.-2.*RG)
      CAP = CEXP(ARG)
      EGH = RG/2./EL
      PHODO = 0.
```

```
      PHOD2 = 2.*PHOD
      CALL VB(RUB1,VUB1,RGH,PHOD0,FN)
      CALL VB(RUB2,VUB2,RGH,PHOD2,FN)
      VBC1 = CMPLX(RUB1,VUB1)
      VBC2 = CMPLX(RUB2,VUB2)
      VBC = VBC1-VBC2
      VD = ANTF*CAP*VAC/(2.*RG)/KP
      RETURN
      END
C
C
C
C
C
      SUBROUTINE FRNELS(C,S,XS)
C!!!
C!!!  THIS IS THE FRESNEL INTEGRAL SUBROUTINE WHERE THE INTEGRAL IS FROM
C!!!  U=0 TO XS, THE INTEGRAND IS EXP(-J*PI/2.*U*U),AND THE OUTPUT IS
C!!!  C(XS)-J*S(XS).
C!!!
      DIMENSION A(12),B(12),CC(12),D(12)
      LOGICAL LTEST,LDEBUG
      COMMON /PIS/PI,TPI,CPR
      COMMON/TEST/LTEST,LDEBUG
      DATA A/1.595769140,-0.000001702,-6.808568854,-0.000576361,6.920691
     *902,-0.016898657,-3.050485660,-0.075752419,0.850663781,-0.02563904
     *1,-0.150230960,0.034404779/
      DATA B/-0.000000033,4.255387524,-0.000092810,-7.780020400,-0.00952
     *0895,5.075161298,-0.138341947,-1.363729124,-0.403349276,0.702222201
     *6,-0.216195929,0.019547031/
      DATA CC/0.,-0.024933975,0.000003936,0.005770956,0.000689892,-0.009
     *497136,0.011948809,-0.006748873,0.000246420,0.002102967,-0.0012179
     *39,0.000233939/
      DATA D/0.199471140,0.000000023,-0.009351341,0.000023006,0.00485146
     *6,0.001903218,-0.017122914,0.029064067,-0.027928955,0.016497308,-0
     *.005598515,0.000838386/
      IF(XS.LE.0.0) GO TO 414
      X=XS
      X = PI*X*X/2.0
      FR=0.0
      FI=0.0
      K=13
      IF(X-4.0) 10,40,40
   10 Y=X/4.0
   20 K=K-1
      FR=(FR+A(K))*Y
      FI=(FI+B(K))*Y
      IF(K-2) 30,30,20
   30 FR=FR+A(1)
      FI=FI+B(1)
      C=(FR*COS(X)+FI*SIN(X))*SQRT(Y)
      S=(FR*SIN(X)-FI*COS(X))*SQRT(Y)
      GO TO 1
   40 Y=4.0/X
   50 K=K-1
```

```
496         FR=(FR+CC(K))*Y
497         FI=(FI+SC(K))*Y
498         IF(K-2) 60,60,50
499  60     FR=FR+CC(1)
500         FI=FI+SC(1)
501         C=0.5+(FR*COS(X)+FI*SIN(X))*SQRT(Y)
502         S=0.5+(FR*SIN(X)-FI*COS(X))*SQRT(Y)
503         GO TO 1
504  414    C=-0.0
505         S=-0.0
506  1      IF(.NOT.LTEST)GO TO 2
507  2      RETURN
508         END
509 C-----------------------------------------------------------------
510         SUBROUTINE VB (RVB,UVB,R,ANGLE,EN)
511 C!!!
512 C!!!   THIS SUBROUTINE IS FOR THE VB CALCULATIONS WHERE RVB IS THE REAL
513 C!!!   PART, UVB IS THE IMAGINARY PART, R IS THE DISTANCE IN WAVELENGTHS.
514 C!!!   ANGLE IS IN DEGREES, AND EN IS N DEFINED BY THE WEDGE ANGLE.
515 C!!!
516         COMPLEX DEA,TOP,CONJEXP,CMPPI,U,PT
517         LOGICAL LTEST,LDEBUG
518         COMMON /PIS/PI,TPI,DPR
519         COMMON/TEST/LTEST,LDEBUG
520         ANG=ANGLE/DPR
521         DEA=CMPLX(0.0,EN*SQRT(TPI))
522         TOP=CEXP(CMPLX(0.0,-(TPI*R+PI/4.0)))
523         CONJ=TOP/DEA
524         ONS=(PI+ANG)/(2.0*EN*PI)
525         SGN=SIGN(1.,ONS)
526         N=IFIX(ABS(ONS)+0.5)
527         ON=SGN*FLOAT(N)
528         A=1.0+COS(ANG-2.0*EN*PI*ON)
529         OTL = 2.0*SQRT(ABS(R*A))
530         EXP=CEXP(CMPLX(0.0,TPI*R*A))
531         CALL FRNELS (C,S,OTL)
532         C=SQRT(PI/2.0)*(0.5-C)
533         S= SQRT(PI/2.0)*(S-0.5)
534         RAG=(PI+ANG)/(2.0*EN)
535         TSIN=SIN(RAG)
536         TS=ABS(TSIN)
537         X=10.)
538         Y=1.0/X**5
539         IF(TS.GT.Y) GO TO 442
540         COMP=-SQRT(2.0)*EN*SIN(ANG/2.0-EN*PI*ON)
541         IF(COS(ANG/2.0-EN*PI*ON).LT.0.0) COMP=-COMP
542         GO TO 443
543  442    UP=SQRT(A)*COS(RAG)/TSIN
544         COMP=UP
545  443    CMPPI=CONJ*EXP*CMPLX(C,S)
546         ONS=(-PI+ANG)/(2.0*EN*PI)
547         SGN=SIGN(1.,ONS)
548         N=IFIX(ABS(ONS)+0.5)
549         ON=SGN*FLOAT(N)
550         A=1.0+COS(ANG-2.0*EN*PI*ON)
```

```
      DUTL = 2.*SQRT(ABS(R*A))
      EXP=CEXP(CMPLX(0.,-.5*PI*R*A))
      CALL ERROR(S (C,S,DUTL)
      C=SQRT(PI/2.0)*(0.5-C)
      S= SQRT(PI/2.0)*(S-0.5)
      ANG=(PI-ANG)/(2.0*PI)
      TSIN=SIN(ANG)
      TS=ABS(TSIN)
      IF(TS.GT.Y) GO TO 542
      COMP= SQRT(2.0)*EN*SIN(ANG/2.0-EN*PI*UN)
      IF(COS(ANG/2.0-EN*PI*UN).LT.0.0) COMP=-COMP
      GO TO 125
  542 OP=SQRT(2)*COS(ANG)/TSIN
      COMPEX=CEXP(OP)
  125 COMPI=CONJG(EXP)*COMP*CMPLX(C,S)
      DVD=REAL (DPI*UNPI)
      DVP=AIMAG(DPI*UNPI)
      IF(.NOT.LTEST)GO TO 1
    1 RETURN
      END
```

REFERENCES

[1] W. H. Peake, "Electromagnetic Scattering from Composite Surfaces," Final Report 4229-2, January 1977, The Ohio State University ElectroScience Laboratory, Department of Electrical Engineering; prepared under Contract N60530-75-C-0216 for Naval Weapons Center, United States Navy, China Lake, California.

[2] W. H. Peake and H. H. Porter, "Physical Optics Back Scatter from a Cylindrical Surface Illuminated by a Nearby Conical Beam Antenna," Report 4229-1, November 1976, The Ohio State University ElectroScience Laboratory, Department of Electrical Engineering; prepared under Contract N60530-75-C-0216 for Naval Weapons Center, United States Navy, China Lake, California.

[3] Encounter Simulation Laboratory Operator Log, 1977.

[4] R. C. Rudduck, "Application of Wedge Diffraction and Wave Interaction Methods to Antenna Theory," Short Course on Application of GTD and Numerical Techniques to the Analysis of Electromagnetic and Acoustic Radiation and Scattering. The Ohio State University Department of Electrical Engineering, September 8-12, 1975.

[5] M. I. Skolnik, Introduction to Radar Systems, McGraw-Hill, New York, 1962, pp. 3-4.